

Multi-isotopic composition (delta Li-7-delta B-11-delta D-delta O-18) of rainwaters in France: Origin and spatio-temporal characterization

Romain Millot, Emmanuelle Petelet-Giraud, Catherine Guerrot, Philippe Négrel

▶ **To cite this version:**

Romain Millot, Emmanuelle Petelet-Giraud, Catherine Guerrot, Philippe Négrel. Multi-isotopic composition (delta Li-7-delta B-11-delta D-delta O-18) of rainwaters in France: Origin and spatio-temporal characterization. Applied Geochemistry, 2010, 25 (10), p.1510-1524. 10.1016/j.apgeochem.2010.08.002 . hal-00553187

HAL Id: hal-00553187
https://brgm.hal.science/hal-00553187

Submitted on 6 Jan 2011

HAL is a multi-disciplinary open access archive for the deposit and dissemination of scientific research documents, whether they are published or not. The documents may come from teaching and research institutions in France or abroad, or from public or private research centers.

L'archive ouverte pluridisciplinaire **HAL**, est destinée au dépôt et à la diffusion de documents scientifiques de niveau recherche, publiés ou non, émanant des établissements d'enseignement et de recherche français ou étrangers, des laboratoires publics ou privés.

Multi-isotopic composition (δ^7Li-δ^{11}B-δD-δ^{18}O) of rainwaters in France: origin and spatio-temporal characterization

Romain Millot[1*], Emmanuelle Petelet-Giraud[2], Catherine Guerrot[1] and Philippe Négrel[1]

1: BRGM, Metrology Monitoring Analysis Department, Orléans, France

2: BRGM, Water Department, Orléans, France

[*] Corresponding author, e-mail: r.millot@brgm.fr, Fax: + 33 2 38 64 37 11

Abstract

Lithium (Li) and boron (B) concentrations and isotope measurements for 45 monthly rainwater samples collected over a 1-year period from four different sites in France, from coastal and inland locations (Brest, Dax, Orléans and Clermont-Ferrand) are reported. This is the first study of Li and B isotope ratios in rainwater samples collected over a long time period at a national scale. The range of Li and B isotopic variations in these rainwaters are measured to enable the determination of the origin of these elements in rainwaters and the characterization of both the seasonal and spatio-temporal effects for δ^7Li and δ^{11}B signatures in rainwaters. Lithium and boron concentrations are low in rainwater samples, ranging from 0.004 to 0.292 µmol/L and from 0.029 to 6.184 µmol/L, respectively. δ^7Li and δ^{11}B values in rainwaters also show a great range of variation between +3.2 and +95.6‰ and between -3.3 and +40.6‰ over a period of one year, respectively, for δ^7Li and δ^{11}B, clearly different from the signature of seawater. Seasonal effects (i.e. rainfall amount and month) is not the main factor controlling element concentrations and isotopic variations. δ^7Li and δ^{11}B values in rainwaters are clearly different from one site to another, indicating the variable contribution of sea salts in the rainwater depending on the sampling site (coastal vs. inland: also called the distance-from-the-coast-effect). This is well illustrated when wind direction data (origin of air masses) is included. We found that seawater is not the main supplier of dissolved atmospheric lithium and boron, and non-sea-salt sources (i.e. crustal, anthropogenic, biogenic) should also be taken into account when Li and B isotopes are considered in hydrogeochemistry as an input to surface waters and groundwater bodies as a recharge. The isotopic variations of the water molecule, vector of the dissolved B and Li, are also investigated and reported as a contour map for δ^{18}O values based on compiled data including more than 400 δ^{18}O values from throughout France. This δ^{18}O map could be used as a reference for future studies dealing with δ^{18}O recharge signature in relation the characterization of surface waters and/or groundwater bodies.

Keywords: lithium isotopes, boron isotopes, hydrogen isotopes, oxygen isotopes, rainwaters, France

8 365 words (without references and captions)

1. INTRODUCTION

Atmospheric aerosols including sea salts, crustal dusts, biogenic materials and anthropogenic emissions are the main sources of chemical elements in rainwaters (Junge 1963). The determination of the chemical composition of rainwater provides an understanding of the source types that contribute to rainwater chemistry and enhances our understanding of the dispersion of elements, whether pollutants or not, and their potential impact on hydrosystems through precipitation and wet deposition processes (Berner and Berner 1987).

The aim of this study is to present the results of the first study of both Li and B isotope ratios in rainwater samples collected over a long time period (i.e. monthly rainfall events over one year, Négrel et al. 2007) at a national scale. In addition, the stable isotopes of the water molecule (δD and δ^{18}O) are also reported here for the same locations (Brest, Dax and Orléans) so that we can discuss the Li and B isotope data in the same context and to provide a framework for the main processes affecting the isotope signatures of the rainwater. Since rainwater is the main input in hydrogeological systems, monitoring the H-O-Li-B isotopic compositions of rainwater at the national scale should enable us to compile a reference system of meteoric isotopic signatures for all of France, as an addition to the Sr isotopes data previously reported by Négrel et al. (2007).

The recent development of new isotopic techniques (e.g. lithium and boron: δ^{7}Li, δ^{11}B) to investigate aquifer systems has highlighted the gap in knowledge of the atmospheric inputs that are the major contributor to groundwater recharge (Widory et al. 2005, Millot et al. 2007). In this context, a knowledge of the spatial and temporal variability of the isotopic compositions of rainwater appears to be essential for hydrogeological investigations and also for sustainable water management.

This paper presents, firstly, the hydrogen and oxygen isotope data from the French Isotopic Data Base (BDISO, 2007), in the form of a contour map linked to data from neighboring countries and, secondly, boron and lithium isotopic data on selected samples from this French monitoring network, part of the international database of the Global Network of Isotopes in Precipitation (GNIP, 2007) managed by the International Agency of the Atomic Energy (IAEA).

The characterization of δ^{7}Li and δ^{11}B signatures in rainwaters is of major importance if we wish to increase our knowledge of the external cycles of these elements and, more specifically in the field of hydrogeochemistry, characterize the Li and B isotope signatures of the rainwater input to surface waters and/or groundwater bodies as a recharge.

To date, one measurement of δ^{7}Li (+14.3‰ ± 0.7) has been reported in the literature for a rainwater event collected in Hawaii (Pistiner and Henderson 2003) and another (+33.3‰),

slightly higher than the seawater signature, for a snow sample collected in Iceland (Pogge von Strandmann et al. 2006).

On the other hand, δ^{11}B signatures of rainwaters are more circumscribed (Miyata et al. 2000, Chetelat et al. 2005, Rose-Koga et al. 2006, Chetelat et al. 2009). Indeed, previous work on the characterization of δ^{11}B signatures in rainwaters have shown that seawater may be a major supplier of atmospheric boron, and that boron isotopic fractionation during evaporation from seawater and removal from the atmosphere may account for the large variations of δ^{11}B signatures observed in the atmosphere and in rainwater (Miyata et al. 2000). In addition, it has been also shown that boron isotopes in rainwater are potentially good tracers of biomass burning (Chetelat et al. 2005) and anthropogenic contamination of the atmosphere in a polluted environment (Chetelat et al. 2009).

The present study aims, therefore, at investigating Li and B isotope signatures in the rainfall input, which should be identified in either surface water or groundwater since the sources of Li and B both are atmospheric, the dissolution of Li- and B-bearing minerals, biogenic and/or anthropogenic. This study also aims to more accurately define the input of Li and B to either surface water or groundwater and place constraints on the δ^{7}Li and δ^{11}B values, which should be corrected for atmospheric input, in order to characterize the anthropogenic signature and/or the signature derived from water-rock interactions.

2. RAINWATER SAMPLES

2.1. Sampling sites

Monthly rain water samples were collected at five different locations throughout France (Brest, Dax, Orléans, Thonon and Avignon, Fig. 1). They constitute the French monitoring network, which is part of the IAEA/IOW Global Network for Isotopes in Précipitation (GNIP 2007) for isotopes of the water molecule. The long-term monthly monitoring consists in sampling rainwater in Avignon (from May-97 to Dec-02, n=60), Brest (from Apr-96 to May-03, n=83), Dax (from Oct-97 to Apr-04, n=74), Orléans (from Mar-96 to May-04, n=96) and Thonon (from Mar-95 to Dec-02, n=89).

Three of these sampling sites were monitored between 2003 and 2004 for B and Li isotopes. One, Brest, is located in the northwest of France (N 48.24, W 04.31), less than 5 km from the Atlantic Ocean. Another, Dax, is located in the southwest of France (N 43.44, W 01.03), 30 km from the Atlantic Ocean. The third, Orléans (N 47.54, E 01.52), is located 400 km from the Atlantic Ocean. A fourth B and Li isotope sampling site is located near Clermont-Ferrand (N 45.46, E 03.04), in the Massif Central, 200 km upstream from Orléans. Rainwater

samples were monitored here between 1994 and 1995. The Mediterranean Sea is 300 km to the south and the Atlantic Ocean is 380 km to the west.

2.2. Sampling technique

A direct polycarbonate funnel (Négrel et al. 1997), 12 cm in diameter and with an area of ~ 110 cm^2, was used to collect the rainfall samples in Brest, Dax and Orléans. This apparatus enables precipitation measurement by direct reading, without the need for preliminary transfer into a measurement test tube. The rainwater was stored in a polypropylene jerrycan to avoid any evaporation or modification of the sample. The accumulation of daily samples enabled a monthly sample of rain to be obtained.

An automatic precipitation sampler was also designed for collecting rainwater samples at the site near Clermont-Ferrand (Négrel and Roy 1998). The basic requirements for our collector were automatic detection and collection of rainfall, elimination of dry fallout, collection of frozen precipitation and prevention of sample contamination. A removable PVC lid covers the funnel when no rain is falling. The cover opens to expose the funnel when electrical contact is made in the rain detector. A polypropylene funnel (45 cm in diameter) was used to collect the rainfall.

After monthly sample collection, 100 mL were used for δD and $\delta^{18}O$ determination. The rest of the rainwater samples were filtered through pre-cleaned 0.45 µm acetate filters using a pre-cleaned Nalgene filter apparatus and the filtrate was separated into two aliquots. From this: (i) 100 and 1000 mL were acidified with double-distilled nitric acid (pH = 2) and stored in pre-cleaned polyethylene bottles for major-cation analysis and lithium isotope ratio and elemental Li and B determinations, and (ii) 500 mL were stored unacidified in polyethylene bottles for anion analysis and B isotope ratio measurements.

3. ANALYTICAL METHODS

3.1. Chemical parameters and stable isotopes of the water molecule

The rainwater samples were chemically analysed by atomic absorption spectrometry (Ca, Na, K, and Mg concentrations, accuracy 5%), ion chromatography (Cl, SO_4 and NO_3 concentrations, accuracy 5%) and inductively coupled plasma mass spectrometry (Li and B concentrations, accuracy 5%). Accuracy and precision for major and trace elements was verified by repeated measurements of standard materials during the course of this study: namely Ion96-3 and LGC6020 for cations and anions and pure Li and B standard solutions (Merck) for Li and B determinations.

Oxygen and deuterium measurements were performed by various French laboratories using a standardised method. At BRGM's laboratory, a Finnigan MAT 252 mass spectrometer was used with a precision of 0.1‰ for $\delta^{18}O$ and 0.8‰ for δD (vs. SMOW). Isotopic compositions are reported in the usual δ-scale (in ‰) according to δ_{sample} (‰) = {($R_{sample}/R_{standard}$) -1} x 10^3, where R is either the $^2H/^1H$ or the $^{18}O/^{16}O$ atomic ratio.

In the present work, it was challenging to measure Li and B isotope compositions in rainwater samples due to their low content (a few µmol/L). We, therefore, developed new sensitive techniques (Millot et al. 2004a, 2004b, Guerrot et al. 2010) in order to be able to accurately and precisely determine δ^7Li and $\delta^{11}B$ for rainwater samples.

3.2. Lithium isotopes

Lithium isotopic compositions were measured using a Neptune Multi Collector ICP-MS (Thermo Fischer Scientific). $^7Li/^6Li$ ratios were normalized to the L-SVEC standard solution (NIST SRM 8545, Flesch et al. 1973) following the standard-sample bracketing method (see Millot et al. 2004a for more details). The analytical protocol involves the acquisition of 15 ratios with 16 s integration time per ratio, and yields in-run precision better than 0.2‰ ($2\sigma_m$, 2 x Standard Error). Blank values are low, (i.e. 0.2%), and 5 minutes wash time is enough to reach a stable background value.

The samples must be prepared beforehand with chemical separation/purification by ion chromatography in order to produce a pure mono-elemental solution. Chemical separation of Li from the matrix was done prior to the mass analysis, following a procedure modified from the technique of James and Palmer (2000), using a cationic resin (a single column filled with 3 mL of BioRad AG® 50W-X12 resin, 200-400 mesh) and HCl acid media (0.2N) for 30 ng of Li. Blanks for the total chemical extraction were less than 30 pg of Li, which is negligible since it represents a 10^{-3} blank/sample ratio.

Successful quantitative measurement of Li isotopic compositions requires 100% Li recovery during laboratory processing. Therefore, frequent column calibration was done and repeated analyses of L-SVEC standard processed through columns shows 100% Li recovery and no induced isotope fractionation due to the purification process.

Accuracy and reproducibility of the entire method (purification procedure + mass analysis) were tested by repeated measurements of a seawater sample (IRMM BCR-403) after separation of Li from the matrix, for which we obtained a mean value of δ^7Li = +30.9‰ $\pm$ 0.4 (2σ, 2 x Standard Deviation, n = 12) over the period of the duration of the analyses. This mean value is in good agreement with our long-term measurement (δ^7Li = +31.0‰ $\pm$ 0.5, 2σ, n = 30, Millot et al. 2004a) and with other values reported in the literature (see, for example,

Tomascak 2004 for a compilation). Consequently, based on long term measurements of the seawater standard, we estimate the external reproducibility of our method to be around ± 0.5‰ (2σ).

In addition, reproducibility of the method was also tested by repeated measurements of a rainwater standard solution (TMRAIN-95, Environment Canada, National Water Research Institute) after separation/purification by ion chromatography, for which we obtained a mean value of δ^7Li = +445.9‰ ± 0.6 (2σ, n = 10) over the period of the duration of the analyses. This mean value could not, however, be compared either to literature data or to certified values because this reference material is not certified for Li isotopes (only for Li concentration). In spite of this, it is of interest to note that this rainwater standard solution is significantly enriched in heavy lithium (^{7}Li). This is, however, not surprising because this reference material is a synthetic rainwater solution (namely: *TMRAIN-95: a simulated rain sample for trace elements*). Consequently, it is likely that lithium in this standard solution could come from an ^{7}Li-rich reagent, as was pointed out by Qi et al. 1997, who showed that δ^7Li values in laboratory reagents could range between -11 and +3013‰. Indeed, it is well known that lithium can be isotopically fractionated due to the removal of ^{6}Li for use in hydrogen bombs. The remaining lithium is therefore substantially enriched in ^{7}Li and some of this lithium has found its way into laboratory reagents and into the environment (Coplen et al. 2002). In addition, we also measured an ICP ^{7}Li-rich standard solution (Spex) that has a mean value of δ^7Li = +241.4‰ ± 0.5 (2σ, n = 38, Millot et al. 2004b), which confirms the results found by Qi et al. 1997.

Finally, concerning the lithium concentration of this rainwater standard solution (TMRAIN-95), we obtained a good agreement between the values measured by ICP-MS in our laboratory (0.059 µmol/L ± 0.003, 2σ n = 10) and the certified value (0.056 µmol/L ± 0.011).

3.3. Boron isotopes

Boron isotope composition were determined following a newly-developed methodology for precise and accurate measurement using a Neptune double-focusing multi-collector sector ICP-MS (Guerrot et al. 2010).

To avoid any drift of the mass bias induced by the sample matrix, chemical purification of 100 ng B was done before the mass analysis, following a procedure described in Guerrot et al. (2010), using the specific boron resin IRA743 and 0.42N HNO_3 acid media with a final boron concentration of 50 ng/mL. ^{11}B/^{10}B ratios were normalized, following the standard-sample bracketing method, to the NIST SRM-951 standard solution (Catanzaro et al. 1970) run through chemistry (Guerrot et al. 2010). Analytical uncertainty for each individual

determination was better than 0.1‰ at $2\sigma_m$ (n = 20). Accuracy and reproducibility of the whole process were determined by repeated measurements of a seawater solution (IAEA-B1) with a mean value of $\delta^{11}B$ = +39.36‰ ± 0.43 (2σ, n = 20). This mean value is in good agreement with our measurements using the positive-TIMS-Cs_2BO_2 technique ($\delta^{11}B$ = +39.24‰ ± 0.36 (2σ, n = 19), as well as with the data compilation obtained for an intercomparison exercise (Gonfiantini et al. 2003) and with the worldwide accepted value for seawater.

Consequently, based on long term measurements of seawater standards, we estimate the external reproducibility of our method around ± 0.5‰ (2σ).

4. RESULTS AND COMMENTS

4.1. Stable isotopes of the water molecule: δD and $\delta^{18}O$

The main processes controlling the $\delta^{18}O$ and δD isotopic signatures in precipitations were summarized by Rozanski et al. (1993): i.e. the rainfall amount, continental and altitude effects and the origins of air masses. The morphology of France is complex with the Massif Central in the centre, the Alps to the East and the Pyrénées to the South, together with the influences of both the Atlantic Ocean and the Mediterranean Sea, which have very different characteristics, as evidenced by Celle-Jeanton et al. (2001) and Ladouche et al. (2009). It is, therefore, of primary importance to constrain the signature of the atmospheric signal in different geographical and geomorphological contexts by means of a rainfall-monitoring network.

The five monitoring stations (Brest, Dax, Orléans, Thonon and Avignon) were selected in order to have a good distribution over the national territory (Fig. 1). This enables, firstly, to follow the evolution of the isotopic signal over a West-East transect from Brest to Thonon via Orléans, and, secondly, to observe the influence of Mediterranean versus Atlantic air masses.

The equation of the Global Meteoric Water Line (GMWL) is $\delta D = 8 \times \delta^{18}O + 10$ (Craig 1961). The arithmetic (unweighted) means of isotopic ratios in precipitation from nearly 410 stations are described by the following equation: $\delta D = 8.07 (\pm 0.02) \times \delta^{18}O + 9.9 (\pm 0.1)$, $R^2 = 0.98$. Long-term means weighted by the amount of precipitation were calculated only for the year for which more than 70% of the rainfall was analysed and at least one year of observation was available (Gourcy et al. 2005). The correlation between the weighted means is: $\delta D_{weighted} = 8.14 (\pm 0.02) \times \delta^{18}O + 10.9 (\pm 0.2)$, $R^2 = 0.98$. When all the available data from the 5 French monitoring stations are plotted in a $\delta^{18}O$ vs. δD diagram (Fig. 2a), the following

equation can be calculated: $\delta D = 7.727 (\pm 0.066) \times \delta^{18}O + 7.033 (\pm 0.451)$, $R^2 = 0.97$, n = 411. When only annual weighted mean values are used for each monitoring station (Fig. 2b), the equation becomes: $\delta D = 8.347 (\pm 0.153) \times \delta^{18}O + 11.662 (\pm 1.048)$, $R^2 = 0.99$, n = 31. These global results are close to the Global Meteoric Water Line despite the variability that can be found at each French station.

The weighted mean for each station integrates all the available data over the monitoring period. The Avignon weighted mean for the period 1997-2002, $\delta^{18}O$ = -5.81‰, is similar to the one calculated during the 1997-1998 period, i.e. $\delta^{18}O$ = -6.1‰ (Celle et al. 2000). These weighted means are reported in figure 3f, in which all points plot very close to the GMWL, and highlight the continental effect (also called the distance-from-the-coast-effect) with progressive depletion in heavy isotopes from Brest (Atlantic coast) to Thonon via Orléans (Fig. 1). It is worth noting that the best fit regression lines of the annual weighted means of these three stations described a quasi-straight line very close to the GMWL (Fig. 2b), suggesting a genetic link of rainfall for the three stations.

In greater detail, the continental effect can be assessed between Brest and Thonon samples (355 km apart) after removing the altitude effect for the Thonon station (at an altitude of 385 m). Blavoux (1978) calculated an altitudinal gradient of -0.3‰/100 m in this region (Chablais, pre-Alpes), leading to a continental effect of -3.2‰ $\delta^{18}O$/1000 km in an eastward direction from the French Atlantic Coast. This value is in good agreement with the assessment of Lécolle (1985) over the French territory. The continental effect varies considerably from place to place and from season to season (Ladouche et al. 2009), even over a low-relief profile. It is also strongly correlated with the temperature gradient and depends on both the topography and the climate regime.

Average annual $\delta^{18}O$ values vary from year to year (Fig. 2b). For the 5 French monitoring stations, the $\delta^{18}O$ values vary between 1 and 2‰ over the monitoring period, as was observed in Wallingford, UK (Darling and Talbot 2003). This is typical of temperate climates where a large part of the spread is caused by variations in the average annual temperature (Gat et al. 2001). These variations from year to year show why it is difficult to assess the real signature of precipitation in a given place without long-term monitoring. This should be kept in mind when drawing a contour map of $\delta^{18}O$ for a vast territory for which only a few long-term monitoring data are available.

4.2. Lithium an boron concentrations in rainwaters

Major elements (cations and anions) and lithium and boron concentrations in rainwater samples collected in Brest, Dax, Orléans and Clermont-Ferrand are given in table 1. When Cl concentrations are plotted as a function of Na concentrations (Fig. 4, Négrel et al. 2007),

we observe a good correlation for the rainwater samples. The regression line between these two major elements is also shown in figure 4. A 95% confidence level is assigned to the data that falls between the two lines. The seawater dilution line is also shown in figure 4. Cl concentrations show a very strong correlation with Na concentrations (R^2 = 0.99). All the samples lie near the seawater dilution line, indicating that both the Na and Cl in these samples come from sea salt. The Brest and the Dax rainwater samples have the highest Na and Cl concentrations, whereas those collected near Clermont-Ferrand have the lowest concentrations in both Na and Cl.

Lithium and boron concentrations in rainwater samples range from 0.004 to 0.292 µmol/L and from 0.029 to 6.184 µmol/L, respectively. This range of variation for Li concentrations is significantly lower than the only other value reported for rainwater (i.e. Li = 0.520 µmol/L, in Hawaii, Pistiner and Henderson 2003). On the other hand, boron concentrations reported in here are in agreement with literature data, with values sometimes higher in the present case (Chetelat et al. 2005, Rose-Koga et al. 2006, Chetelat et al. 2009).

Li concentrations are more homogeneous than boron concentrations from one sampling site to another. The mean lithium concentration values for the various sites are quite similar (0.058, 0.066, 0.053 and 0.057 µmol/L for rainwaters collected at Brest, Dax, Orléans and near Clermont-Ferrand, respectively), whereas they are more heterogeneous for boron (i.e. 0.66, 0.90, 1.51 and 0.20 µmol/L for rainwaters collected at Brest, Dax, Orléans and near Clermont-Ferrand, respectively).

The overall range of variation for Li and B concentrations can be seen in figure 5a and 5b, where lithium and boron concentrations are plotted as a function of the Na concentrations as seasalt tracer (Négrel and Roy, 1998). Again, we see that these rainwater samples are rather homogenous for lithium concentrations (with the exception of 2 Li-rich samples). Moreover, it appears that rainwaters are slightly enriched in Li and B compared to Na derived from seawater. No correlation could be found, however, between Li and B concentrations in rainwater samples (Fig. 5c).

4.3. Lithium and boron isotopes

Lithium and boron isotope compositions are reported in table 1 and figure 6. The most striking outcome of this study is that there is a very large range of variation (between +3.2 and +95.6‰) for δ^7Li in rainwaters. Mean δ^7Li values are +22.5, +22.8, +16.1 and +26.2‰ for samples collected in Brest, Dax, Orléans and near Clermont-Ferrand, respectively. This range of variation is consistent with the only other value reported for rainwater (δ^7Li =

+14.3‰, in Hawaii, Pistiner and Henderson, 2003). Furthermore, δ^7Li values in rainwaters are significantly different from the δ^7Li signature of seawater (+31‰, Millot et al. 2004a).

δ^{11}B in rainwaters also shows a very wide range of variation, between -3.3 and +40.6‰. The mean δ^{11}B values are +37.4, +11.4, +8.4 and +23.2‰ for rainwaters collected in Brest, Dax, Orléans and near Clermont-Ferrand, respectively. This is in agreement with literature data (Chetelat et al. 2005, Rose-Koga et al. 2006, Chetelat et al. 2009) and is significantly different from the δ^{11}B signature of seawater (+39.5‰, see data compilation reported by Aggarwal et al. 2004), except for Brest.

In figures 7a and 7b, δ^7Li and δ^{11}B values are plotted as a function of Li and B concentrations, respectively. No general correlation is observed between δ^7Li and Li concentrations (Fig. 7a). Indeed, the range of δ^7Li variation is covered at both low and high Li concentrations (with the exception of the three ^{7}Li-rich samples from Clermont-Ferrand). On the other hand, there seems to be an inverse correlation between δ^{11}B and B concentrations (Fig. 7b). Initially high δ^{11}B values (close to seawater signature, i.e. corresponding to rainwater samples from Brest, which is near the ocean) tend to decrease down to nearly -3‰ as B concentrations increase. This also means that high B concentrations in rainwaters are associated with low δ^{11}B values, especially for Orléans rainwater samples.

The overall range of variation for both δ^7Li and δ^{11}B values is very great (over 90‰ and 40‰, respectively, for δ^7Li and δ^{11}B, Fig. 6), and these isotopic signatures for rainwater samples are significantly different from the isotopic signature of seawater (+31.0 and +39.5‰, respectively, for δ^7Li and δ^{11}B values). Seawater might, therefore, be a major source of dissolved atmospheric lithium and boron (especially for rainwater collected near the ocean), but other sources must also be considered.

5. DISCUSSION

5.1. Contour map of the stable isotopic signature of oxygen (δ^{18}O)

The world map developed by the IAEA from GNIP data (GNIP 2007) is one of the few contour maps of the stable atmospheric signal that exist today. In France, a δ^{18}O contour map was drawn by Lécolle (1985), based on the oxygen isotopic composition of the carbonate shell of landsnails, which have been shown to be directly linked to the annual mean δ^{18}O of rainwater. A second map, based on a few rainwater and groundwater measurements, was drawn by Razafindrakoto (1988).

In the present work, the stations in Brest, Dax, Orléans, Avignon and Thonon (Fig. 1) were monitored monthly for the $\delta^{18}O$ and δD atmospheric signal. Rain samples from the BDISO databank are from studies dedicated to the knowledge and functioning of specific aquifers, often represent only a few months of monitoring, and are not for the same time periods. From all the available data, we selected data points with the following criteria: (1) there must be at least one year of monitoring; (2) isotopic data should be associated with the rainfall amount (if rainfall values are unavailable, data are weighted by those from the nearest meteorological station at the same altitude); (3) when two points are close, only the longest and more recent monitoring campaign is selected, as well as the lowest altitude point to minimize the altitude effect when drawing the map. Rain data from 44 points were selected (Fig. 8). Some regions are poorly documented and additional data were selected. In the Southwest of France, lakes considered to be natural rain gages under well-defined conditions (lakes in pristine environments located in the upper parts of drainage basins to limit runoff, Petelet-Giraud et al. 2005) are used after data has been corrected for evaporation. Data from 13 lakes were used. In other regions, recent groundwater (i.e. Tritium values >0 and ^{14}C Activity close to 100%) was used as a reference material as it has been shown to be often reasonably representative of long-term rainfall (Darling et al. 2003). Data for 12 groundwater bodies were used. No data are available for the Rhône River Valley. We, therefore, used a signature calculated from that of a landsnail shell from the Northern part of the valley (Lécolle 1985). To better determine the isotopic signature at the French border, we used data from the literature or long-term rain monitoring data in the GNIP database for neighbouring countries (GNIP 2007, Plata-Bedmar 1994, Longinelli and Selmo 2003, Longinelli et al. 2006, Darling and Talbot 2003, Darling et al. 2003, Schurch et al. 2003).

The contour map of $\delta^{18}O$ values was drawn manually for the following reasons: (1) to take into account the altitude from the topographic digital terrain model (DTM) for a better interpolation, reflecting the altitude affect and (2) to give a greater weight to the most representative samples (length of the monitoring campaign, altitude, etc.) when large isotopic variations were observed at small scale. Our attempts to automatically generate the map with dedicated software with kriging methods were rather inconclusive mainly because, as the data including the altitude effect, it was impossible to take into account the DTM in the interpolation without a risk of taking the altitude effect into account twice.

The resulting map of the meteoric $\delta^{18}O$ signal (Fig. 8) clearly shows the main effects that could affect the isotopic signature of rainwater. The continental and altitude effects are clearly visible. It is also in good agreement with the map drawn by Lécolle (1985), with a high degree of precision, especially in the North. The new contour map still remains quite schematic because of the limited number of available data points and the complexity of the French topography. This is especially true in mountainous regions, where the density of data

is too low and the relief too uneven for us to draw reliable lines. $\delta^{18}O$ iso-value lines are, therefore, represented by dotted lines in the Pyrénées and the Alps.

The map also shows that the signature along the Atlantic coast is relatively homogeneous with a $\delta^{18}O$ value of around -5‰, despite the difference in latitude and the known climatic differences. The same phenomenon is observed on the Mediterranean coast of Italy (Longinelli and Selmo 2003) and can be at least partially related to the contribution of seawater vapor to the coastal precipitation, with values characteristic of a first condensate of vapor (Gat et al. 2001). While the isotopic signal on the Mediterranean coast is not significantly different from that on the Atlantic coast, the Mediterranean signature is more rapidly depleted in heavy isotopes as we move inland from the coast. This could be due to the presence of mountains close to the coast, which generate rainfall. Rainwater in and around Paris is less depleted in heavy isotopes than available data indicates for the surrounding area. This might be explained by a slightly higher temperature induced by the high population density and intensive industrial activity. Such a phenomenon has been described in Rome (Italy) (Longinelli and Selmo 2003). The Northern coast presents a $\delta^{18}O$ signal, depleted in heavy isotopes compared to the Atlantic coast (-6.5‰ vs. -5.3‰ in Brest and -5.6‰ in Dax), which suggests that clouds that produce rainfall are already depleted in heavy isotopes. This phenomenon has been observed over the British Isles. The $\delta^{18}O$ contour lines are parallel on each side of the Chanel.

This map is the first one drawn at the national scale based on most of the isotopic data available in France, and which takes into account data for neighbouring countries in order to better constrain the contour lines along the borders. It is, therefore, a unique tool for assessing the stable isotopic signature of aquifer recharge for oxygen isotopes. Nevertheless, it is worth noting that the rainwater data used often integrate only one year of rainfall and we have shown that the mean annual weighted $\delta^{18}O$ values vary from 1 to 2‰ due to variations in the average annual temperature typical of temperate climates. This map can, therefore, be a valuable addition to local rain monitoring when a specific aquifer is being studied.

In this paper, we report only the $\delta^{18}O$ signature for France. However, δD can be determined using the global correlation between δD and $\delta^{18}O$ (the Global Meteoric Water Line) since all the data considered plot, for the most part, along this line.

5.2. Lithium and boron isotopes variations

5.2.1. Seasonal and spatio-temporal variations

Monitoring rainwater samples over a period of one year at different locations allows us to study seasonal effects on the range of variation for both Li and B isotopes. We have plotted Li and B isotopes as a function of the rainfall amount (mm) (Figs. 9a and b) and the month (Figs. 9c and d). The rainfall amount seems to have no effect on δ^7Li variations (Fig. 9a). The total range of variation for δ^7Li values seems to be independent of the rainfall amount, and this is especially true for Orléans, Brest and Dax. On the other hand, for Brest and Dax samples (sampling points on or near the coast), the rainfall amount does seem to control δ^{11}B variations to some extent (Fig. 9b). When the rainfall amount increases, the δ^{11}B values increase for the Brest samples but decrease for the Dax samples. It is very likely that when the rainfall amount is great, there is a large contribution of sea salts derived from seawater. This is especially true for the Brest rainwater samples (sampling point less than 5 km from the Atlantic Ocean). However, the trend observed for δ^{11}B the rainwater samples from Dax (30 km inland) is more complex. We know that, in this area, rainfall comes not only from the Atlantic Ocean to the West, but also from the Pyrénées Mountains to the South. Therefore, we can assume that for the Dax rainwater samples: (i) during the summer and winter (low rainfall amount), δ^{11}B is controlled mainly by the sea salt contribution coming from the Atlantic Ocean, whereas (ii) during spring and autumn when rainfall is heavier, δ^{11}B might also be controlled by rain coming from the mountains that has been in contact with local dust (i.e. silicate, carbonate and/or evaporite particulates from the Pyrénées), lowering δ^{11}B values. In addition, like Négrel et al. (2007) have observed for Sr isotopes at the same sampling site, biogenic sources might also contribute to the δ^{11}B signature of the Dax samples, also lowering the δ^{11}B values. Indeed, Dax is located in a huge maritime pine forest (*Pinus pinaster*) that covers 860,000 hectares, the trees growing in sand containing chlorite, micas, feldspars and quartz (Righi and De Connick 1977).

Rainwater samples from inland sampling points (Orléans and Clermont-Ferrand) do not show any correlation of δ^{11}B values with the rainfall amount (Fig. 9b). Likewise, the month does not appear to have any effect on δ^7Li values (Fig. 9c). However, ^{7}Li-rich values for Clermont-Ferrand rainwater are observed during the winter and spring seasons (December, February and April).

There appears to be no correlation between δ^{11}B values and the month (Fig. 9d). The range of variation for δ^{11}B is controlled, first of all, by the location (inland vs. coastal) of the sampling point.

5.2.2. Wind direction and air mass origin

The origin of the air masses for the French rainwater under consideration was studied using the French Meteorological Institute database (www.meteofrance.com). Daily maximum wind direction (0 to 360°) and rainfall (mm) were considered. Average monthly wind direction data are given in table 1 for each sampling point. These average values were calculated by weighting daily maximum wind directions by the corresponding rainfall amount and only rainy days were considered.

The effect of wind direction, and thus the origin of the air masses, at each sampling site was investigated by identifying correlations between wind direction and Li-B concentrations and their isotopes.

5.2.2.1. Lithium

Li concentrations and δ^7Li values were plotted as a function of the wind direction (Fig. 10). The wind direction does not control Li content in Brest and Clermont-Ferrand rainwater samples (Figs. 10b and 10h). For Dax and Orléans sampling sites, however, there is a correlation between Li concentration and wind direction (Figs. 10d and 10f). The lithium concentration is controlled by the origin of the air masses for these rainwater samples, with higher Li concentrations in rainwater coming from the ocean (wind direction around 270°, i.e. W). Concerning δ^7Li values, no effect is observed, here again, for Brest rainwaters (Fig. 10a), which means that most of rainwater at this site is homogeneous for both Li and its isotopes, even though the wind direction can range significantly (from 50 to 240°, i.e., NE to WSW). For Dax and Orléans samples, opposite phenomena are observed concerning Li isotopes. When the air masses have a Western origin (oceanic input), δ^7Li values tend to increase slightly for Dax rainwaters but decrease slightly for Orléans rainwaters (Figs. 10c and 10e). The most striking observation concerns Clermont-Ferrand rainwaters, for which δ^7Li values display two interesting trends as a function of the wind direction (Fig. 10g). In winter and spring samples, there is a positive correlation between δ^7Li and wind direction. However, autumn and summer samples show no change in the δ^7Li signature when the wind direction is between 120 and 300°. This means that the ^{7}Li-rich rainwaters are characterized by air masses coming from SSW of the sampling site during the winter and spring.

5.2.2.2. Boron

B concentrations and δ^{11}B values were plotted as a function of the wind direction (Fig. 11). B concentrations in Brest and Clermont-Ferrand rainwaters are not controlled primarily by the wind direction (Figs. 11b and 11h, respectively). However, for Dax and Orléans rainwaters, B

concentrations increase when the wind comes from West of the sampling site (marine origin, Figs. 11d and 11f). There is no evidence that $\delta^{11}B$ values in Brest and Clermont-Ferrand rainwaters are controlled by the wind direction (Figs. 11a and 11g), whereas $\delta^{11}B$ values in Dax rainwaters increase when the wind direction ranges from 210° (SW) to 270° (W) (Fig. 11c), in agreement with our conclusions in section 5.2.1. concerning the two major origins of boron at this site (sea salt from the Atlantic Ocean (W) and rainfall from the Pyrénées (SW) having lower $\delta^{11}B$ values). $\delta^{11}B$ values in rainwater in Orléans decrease slightly when the wind direction ranges from 180° (S) to 270° (W) (Fig. 11e).

The origin of the air masses is, therefore, an important factor that can control the dissolved concentration of Li and B for the Dax and Orléans sampling sites, but seems to have no effect on Clermont-Ferrand and Brest rainwaters. This is probably due to the homogeneity of the rainfall for the Brest sampling site. On the other hand, for Dax, rainwater could have two main origins – the SSW (with lower $\delta^{7}Li$ and $\delta^{11}B$ values) or the W (with higher $\delta^{7}Li$ and $\delta^{11}B$ values), which reflects the contribution of marine sea salts. For Clermont-Ferrand, the wind direction has no significant effect on either Li or B concentrations, whereas we have seen that the ^{7}Li-rich rainwaters are characterized by air masses coming from the SSW of the sampling site during the winter and spring.

The spatial range of variation for Li and B isotopes could then be studied because we monitored rainwater samples at different locations in France (coastal and inland). The rainwaters sampled at Brest, near the sea, have both $\delta^{7}Li$ and $\delta^{11}B$ values close to the seawater signature (Figs. 6 and 12), whereas those sampled at Dax, Orléans and Clermont-Ferrand have a very broad range of variation for both $\delta^{7}Li$ and $\delta^{11}B$ values – from crustal values (i.e. from -2 to +2‰ and from -5 to +10‰, respectively, for $\delta^{7}Li$ and $\delta^{11}B$, Teng et al. 2004, Tomascak 2004, Barth 1993, Barth 2000 and Millot et al. 2007) up to the $\delta^{7}Li$ and $\delta^{11}B$ signatures of seawater (+31.0 and +39.5‰, respectively, for $\delta^{7}Li$ and $\delta^{11}B$). However, higher $\delta^{7}Li$ values are measured in some rainwater samples collected near Clermont-Ferrand. We, therefore, discuss below the origins of lithium and boron in rainwaters, and the associated isotope signatures, that might explain the observed range of variation for both Li and B isotope systematics.

5.3. Origin of lithium and boron in rainwaters

Seawater (by contributing sea salts) might be one of the major suppliers of atmospheric lithium and boron, but other sources must also to be taken into account. We, therefore, determined the contribution of sea salts to lithium and boron in rainwater samples.

Na concentrations in rainwater samples can be used to estimate the sea salt contribution of other ions because Na is the best tracer of sea salt input in rainwater (Keene et al. 1986, Négrel and Roy 1998, Basak and Alagha 2004, Rastogi and Sarin 2005). Distinguishing between the sea salt (ss) and non-sea salt (nss) component contributions in rainwater (rw) is essential if we wish to characterize the chemistry of precipitation (Négrel and Roy 1998, Schmitt and Stille 2005, Al-Khashman 2005, Rastogi and Sarin 2005, Négrel et al. 2007).

To calculate the contribution of Li and B (X in equation 1) in the sea salt component (ss) with seawater (sw) characteristics, the following equation is used:

$$X_{ss} = Na_{rw} \times \left(\frac{X}{Na} \right)_{sw} \quad (1)$$

Na is used as a marine tracer in rainwater (see Négrel and Roy 1998 and references therein). The contribution of the non-sea salt component (nss) is the difference between the total composition of rainwater (rw) and the sea salt (ss) contribution:

$$X_{nss} = X_{rw} - X_{ss} \quad (2)$$

This equation enables us to determine the contribution of sea salts for lithium and boron concentrations in rainwaters (Fig. 13). Results show that the contribution of sea salt for boron concentrations in rainwaters is greater than for lithium concentrations. Indeed, considering average values for the 4 different sampling sites, we see that the marine contribution (sea salt) to B in rainwaters is twice that to Li (22.3% and 12.0%, respectively, Fig. 13). The distance-from-the-coast-effect (inland vs. coastal location) is the key parameter controlling the marine contribution for both Li and B to rainwater concentrations. Samples collected inland (Orléans and Clermont-Ferrand) show the lowest sea salt contributions. Rainwaters from Dax have intermediate values (Fig. 13), whereas rainwaters collected at Brest have the highest contributions of marine sea salt to Li and B concentrations (25% and 49.8% on average, respectively, for Li and B).

Although these results are not surprising, they show that although seawater does, indeed, supply dissolved atmospheric lithium and boron, non sea salt sources represent the major source of Li and B in rainwaters.

This could be of importance in hydrogeochemical studies of surface water and groundwater bodies because rainwater is an input for the former and a recharge for the latter. The non sea salt signature for Li and B isotopes should, therefore, be taken into consideration for future studies in the investigation of their isotope systematics in water.

5.4. Lithium isotopes in rainwaters

The fact that most of dissolved Li in rainwaters does not have a marine origin is in agreement with the range observed in δ^7Li in our samples (+3.2 and +95.6‰) compared to the marine signature of Li isotopes (~ +31‰).

δ^7Li values in rainwater samples were plotted as a function of Li derived from sea salt (Fig. 14a) in an attempt to identify the different sources contributing to the rainwaters Li isotopes signature. For rainwater sampled at a coastal location (Brest), the marine contribution is relatively great (9 to 45%), but another source or other sources is/are needed in order to explain the range of variation in these δ^7Li values (+15.1 to +28.6‰). The same is observed for rainwaters collected at Dax and Orléans, but at these locations the non sea salt contribution should be even greater since these sites are located inland (especially Orléans) and show lower marine contributions. The dissolution of either Li-bearing minerals or anthropogenic inputs might explain lower δ^7Li values compared to the seawater signature (~ +31‰).

Continental rocks have δ^7Li values ranging from -4 to +8‰ (Teng et al. 2004 and references therein) and might contribute to rainwater signatures by interaction in the atmosphere between continental particles and water molecules. In addition, most carbonates analysed to date show δ^7Li values between +6 and >25‰ (e.g. Hoefs and Sywall 1997, Hall et al. 2005, Hathorne and James 2006, Vigier et al. 2007) and could also be cited there. It is, however, more likely that multiple sources exist for the crustal component at the scale of France.

The three rainwater samples from Clermont-Ferrand having a ^{7}Li-rich signature (δ^7Li values of +63.8, +77.6 and +95.6‰) are, however, notable because they have significantly heavier Li isotopic compositions than seawater. Négrel and Roy (1998) and Roy and Négrel (2001) have shown that rainwater in this area is likely to record an anthropogenic input due to agricultural activities (e.g. fertilizers application). These high δ^7Li values might, therefore, be explained by the contribution of a local input derived from fertilizers and/or soil amendments used by farmers in this area. This is also in good agreement with recent results of Négrel et al. (2009) concerning the Li isotopic characterization of a peat bog located near our sampling site. In this study, the ^{7}Li-rich contribution to surface waters is explained by the dissolution of fertilizers and soil amendments having δ^7Li values higher than +215‰ (Négrel et al. 2009). This heavy lithium component is attributed to synthetic Li added into fertilizers and soil amendments, derived from a ^{7}Li-rich reagent, as was reported by Qi et al. (1997). In addition, we have seen (section 5.2.2) that these ^{7}Li-rich rainwaters are characterized by air masses coming from the SSW of the sampling site during the winter and spring, which is when soils are fertilized and amended.

When Li isotopes are plotted as a function of the Na/Li molar ratio (Fig. 15), we observe that samples from Clermont-Ferrand seem to indicate a mixing of a crustal component (granite and/or carbonate) and an anthropogenic component (^{7}Li-rich end-member), whereas samples from Brest, Dax and Orléans seem to indicate a mixing of a crustal component (complex due to the relative contribution of different particles derived from carbonate or granite) and a marine end-member.

5.5. Boron isotopes in rainwaters

As stated above, most of the dissolved B in rainwater is not of marine origin (for rainwater samples collected at inland locations in Orléans and Clermont-Ferrand, in particular). This is in agreement with the range observed in δ^{11}B values in our samples (-3.3 and +40.6‰) compared to the marine signature of B isotopes (+39.5‰, Aggarwal et al. 2004 and data therein).

δ^{11}B values in rainwater samples have been plotted as a function of B derived from sea salt (Fig. 14b). Seawater seems, nevertheless, to be a major supplier of rainwater boron in Brest, near the ocean. However, the rainwater sample collected at Brest in August 2003 is notable (the lowest δ^{11}B value: +27.5‰). It was collected at a time when France and Western Europe were having an exceptionally severe heat wave with record temperatures and little rainfall (Luterbacher et al. 2004, Chase et al. 2006), and it is very likely that this sample is not representative.

Concerning the Dax, Orléans and Clermont-Ferrand rainwater samples, another source or other sources is/are needed in order to explain the range of variation in δ^{11}B values. As for lithium, the dissolution of either B-bearing minerals or anthropogenic inputs might explain δ^{11}B values lower than the seawater signature (+39.5‰). A crustal component probably contributes to rainwater signatures by the interaction in the atmosphere of continental particles and water molecules. B isotopic compositions for the main crustal lithologies have been well identified, with δ^{11}B values ranging from -5 to +10‰, from +15 to +30‰ and from 0 to +35‰, for granite and gneiss, marine evaporite and carbonate, respectively (Barth 1993, 2000). This crustal component is expected to contribute to the B isotopic rainwater signature, although the crustal component is probably made up of a combination of several sources (different particles coming from different lithologies).

Plotting B isotopic compositions as a function of NO_3/B molar ratios (NO_3 being a good tracer of fertilizer) provides additional and important information (Fig. 16). Samples from Dax, for which we have already suggested a possible biogenic input, are in agreement with field data reported by Chetelat et al. (2005) for the biomass-derived end-member (this is also true for

most samples from Orléans, located near a large forested area, “La Sologne”, an area covering 500,000 ha). In addition, the B values in rainwaters from this study are little affected by anthropogenic emissions compared to those of rainwater sampled in Paris that have an urban aerosol component (Chetelat et al. 2009). Most rainwater samples from Clermont-Ferrand (for which we have cited a possible fertilizer input based on Li isotope data) also reveal a mixing trend toward a fertilizer end-member (Fig. 16) based on B isotopes tracing.

6. CONCLUSIONS

This work has made it possible to better characterize Li, B, H and O isotopes in rainwaters. The main results of this study are:

• Li and B concentrations and δ^{7}Li and δ^{11}B signatures in rainwater samples collected over one year in four stations (Brest, Dax, Orléans and Clermont-Ferrand) varied greatly over the sampling period.

• Lithium and boron concentrations are low and comprised between 0.004 and 0.292 µmol/L and 0.029 and 6.184 µmol/L, respectively.

• δ^{7}Li and δ^{11}B values in rainwaters also vary greatly between +3.2 and +95.6‰ and -3.3 and +40.6‰ over a period of one year, respectively.

• The seasonal effect (i.e. the month or rainfall amount) is not the main controlling factor for these isotopic variations. However, the continental effect (distance from the coast) is a key parameter, determining the origin of both lithium and boron derived from marine sea salts. In addition, the origin of air masses (wind direction) is also a key parameter that controls the contribution of sea salts derived from the Ocean.

• The most striking outcome of this study is that most lithium and boron in rainwaters does not have a marine origin. Seawater is not the major supplier of atmospheric lithium and boron and a non-sea-salt source, such as a crustal component and/or an anthropogenic contribution, should also be taken into account when Li and B isotopes are studied in hydrogeochemistry as an input to surface waters and a recharge to groundwater bodies. This may be important in the understanding of dissolved Li and B distributions in ground- and formation waters, and should be taken into account in future studies.

• A contour map of France for δ^{18}O was drawn after compiling data that included more than 400 values from all of France. This map could be used as a reference for future studies concerning the recharge δ^{18}O signature in surface water and groundwater body characterization. It represents a unique tool for assessing the stable isotopic signature of the recharge of aquifers for oxygen isotopes.

Acknowledgements

This work was funded by the Research Division of the BRGM. The authors thank all the people who have contributed to the French Isotopic Data Base (BDISO) through their technical assistance, sampling and isotopic measurements: University of Paris-Sud (Orsay), University of Avignon, Centre de Recherches Géodynamiques (Thonon-les-Bains), CEA (Saclay) and BRGM in Orléans. BDISO aims at gathering isotopic data (mainly $\delta^{18}O$, δD, ^{3}H, ^{14}C, $\delta^{13}C$, $^{87}Sr/^{86}Sr$, $\delta^{11}B$ and $\delta^{15}N$) on French groundwater, surface water and rainwater. We thank J. Garnier for compiling most of the $\delta^{18}O$ and δD data and drawing the first version of the $\delta^{18}O$ contour map presented here. We thank Météo France (Direction de la Production) for providing the wind direction and rainfall data. This work benefited from the collaboration of BRGM's chemistry laboratories for major and trace element analyses: J.P. Ghestem, T. Conte and C. Crouzet are thanked for their help, as well as C. Fléhoc for stable isotope measurements (δD and $\delta^{18}O$). We also would like to thank M. Robert for her help in the Neptune laboratory. This is BRGM contribution n° XXXX.

References

Aggarwal J.K., Mezger K., Pernicka E., Meixner A. (2004) The effect of instrumental mass bias on δ^{11}B measurements: a comparison between thermal ionisation mass spectrometry and multiple-collector ICP-MS. International Journal of Mass Spectrometry, 232: 259-263.

Al-Khashman O.A. (2005) Ionic composition of wet precipitation in the Petra Region, Jordan. Atmospheric Research, 78: 1-12.

Barth S.R. (1993) Boron isotope variations in nature: a synthesis. Geol. Rundsch, 82: 640-641.

Barth S.R. (2000) Geochemical and boron, oxygen and hydrogen isotopic constraints on the origin of salinity in groundwaters from the crystalline basement of the Alpine Foreland. Applied Geochemistry, 15: 937-952.

Basak B., Alagha O. (2004) The chemical composition of rainwater over Büyükçekmece Lake, Istanbul. Atmospheric Research, 71: 275-288.

BDISO (2007) French Isotopic Data Base on groundwater, surface water and rainwater. Available at: http://infoterre.brgm.fr/eSIG/index.jsp

Berner E.K., Berner R.A. (1987) The global water cycle. Geochemistry and Environment. Prentice-Hall, 394 p.

Blavoux B. (1978) Etude du cycle de l'eau au moyen de l'oxygène 18 et du Tritium. Possibilités et limites de la méthode des isotopes en milieu en hydrologie de la zone tempérée. Thèse d'Etat, Université Paris VI, France.

Catanzaro E.J., Champion C.E., Garner E.L., Marinenko G., Sappenfield K.M., Shields W.R. (1970) Standard reference materials: Boric acid; isotopic and assay standard reference materials. US National Bureau of Standards, Special Publication 260-17, 70pp.

Celle H., Daniel M., Mudry J., Blavoux B. (2000) Signal pluie et traçage par les isotopes stables en Méditerranée occidentale. Exemple de la région avignonnaise (Sud-Est de la France). Comptes Rendus de l'Académie des Sciences Paris, 331: 647-650.

Celle-Jeanton H., Travi Y., Blavoux B. (2001) Isotopic typology of the precipitation in the Western Mediterranean region at three different time scales. Geophys. Res. Lett., 28: 1215-1218.

Chase T.N., Wolter K., Pielke R.A, Rasool I. (2006) Was the 2003 summer European heat wave unusual in a global context? Geophys. Res. Lett., 33: L23709.

Chetelat B., Gaillardet J., Freydier R., Négrel, Ph. (2005) Boron isotopes in precipitation: experimental constraints and field evidence from French Guiana. Earth Planet. Sci. Lett., 235: 16-30.

Chetelat B., Gaillardet J., Freydier R. (2009) Use of B isotopes as a tracer of anthropogenic emissions in the atmosphere of Paris, France. Applied Geochemistry 24: 810-820.

743 Coplen T.B., Hopple J.A., Böhlke J.K., Peiser H.S., Rieder S.E., Krouse H.R., Rosman
744 K.J.R., Ding T., Vocke R.D.Jr., Révész K.M., Lamberty A., Taylor P., De Bièvre P. (2002)
745 Compilation of minimum and maximum isotope ratios of selected elements in naturally
746 occurring terrestrial materials and reagents. U.S. Geological Survey, Water-Resources
747 Investigations, Report 01-4222.
748 Craig H. (1961) Isotopic variations in meteoric waters. Science, 133: 1702-1703.
749 Darling W.G., Talbot J.C. (2003) The O and H stable isotopic composition of fresh waters in
750 the British Isles. 1. Rainfall. Hydrology and Earth System Sciences, 7: 163-181.
751 Darling W.G., Bath A.H., Talbot J.C. (2003) The O and H stable isotopic composition of fresh
752 waters in the British Isles. 2. Surface waters and groundwater. Hydrology and Earth
753 System Sciences, 7: 183-195.
754 Flesch G.D., Anderson A.R., Svec H.J. (1973) A secondary isotopic standard for $^{6}Li/^{7}Li$
755 determinations. International Journal of Mass Spectrometry and Ion Physics, 12: 265-272.
756 Gat J.R., Mook W.G., Meijer H.A.J. (2001) Volume II: Atmospheric Water. In: Mook, W.G.
757 (Eds), Environmental Isotopes in the hydrological cycle. Principles and applications. IHP-V
758 Technical Documents in Hydrology, Nº 39. UNESCO-IAEA.
759 GNIP (2007) Global Network of Isotopes in Precipitation. Available at: http://isohis.iaea.org/
760 Gonfiantini R., Tonarini S., Gröning M., Adorni-Braccesi A., Al-Ammar A.S., Astner M.,
761 Bächler S., Barnes R.M., Bassett R.L., Cocherie A., Deyhle A., Dini A., Ferrara G.,
762 Gaillardet J., Grimm J., Guerrot C., Krähenbühl U., Layne G., Lemarchand D., Meixner A.,
763 Northington D.J., Pennisi M., Reitznerová E., Rodushkin I., Sugiura N., Surberg R., Tonn
764 S., Wiedenbeck M., Wunderli S., Xiao Y., Zack T. (2003) Intercomparison of boron isotope
765 and concentration measurements. Part II: Evaluation of results. Geostandards Newsletter:
766 The Journal of Geostandards and Geoanalysis, 27, 1: 41-57.
767 Gourcy L., Groening M., Aggarwal P.K. (2005) Stable oxygen and hydrogen isotopes in
768 precipitation. In: P.K., Aggarwal, J.R. Gat and K.F.O. Froehlich (eds), Isotopes in the
769 Water Cycle: Past, Present and Future of the Developing Science, 39-51.
770 Guerrot C., Millot R., Robert M., Négrel Ph. (2010) Accurate and high-precision
771 determination of boron isotopic ratio by MC-ICP-MS Neptune. Geostandards and
772 Geoanalytical Research, in revision.
773 Hall J.M. , Chan L.H., McDonough W.F., Turekian K.K. (2005) Determination of the lithium
774 isotopic composition of planktic foraminifera and its application as a paleo-seawater proxy.
775 Marine Geology, 217: 255-265.
776 Hathorne E.C., James R.H. (2006) Temporal record of lithium in seawater: A tracer for
777 silicate weathering? Earth and Planetary Science Letters, 246: 393-406.

778 Hoefs J., Sywall M. (1997) Lithium isotope composition of Quaternary biogene carbonates
779 and a global lithium isotope balance. Geochimica et Cosmochimica Acta, 61: 2679-2690.
780 James R.H., Palmer M.R. (2000) The lithium isotope composition of international rock
781 standards. Chemical Geology, 166: 319-326.
782 Junge C. E. (1963) Air chemistry and radioactivity. NewYork, Academic Press.
783 Keene W.C., Pszenny A.A.P., Galloway J., Hawley M.E. (1986) Sea-salt corrections and
784 interpretation of constituent ratios in marine precipitation. Journal Geophysical Research,
785 91: 6647-6658.
786 Ladouche B., Aquilina B., Dörfliger, N. (2009) Chemical and isotopic investigation of
787 rainwater in Southern France (1996-2002): Potential use as input signal for karst
788 functioning investigation. Journal of Hydrology, 367: 150-164.
789 Lécolle P. (1985) The oxygen isotope composition of landsnail shells as a climatic indicator:
790 applications to hydrogeology and paleoclimatology. Chemical Geology, 58: 157-181.
791 Longinelli A., Selmo E. (2003) Isotopic composition of precipitation in Italy: a first overall
792 map. Journal of Hydrology, 270 : 75-88.
793 Longinelli A., Anglesio E., Flora O., Iacumin P., Selmo E. (2006) Isotopic composition of
794 precipitation in Northern Italy: Reverse effect of anomalous climatic events. Journal of
795 Hydrology, 329: 471-476.
796 Luterbacher J., Dietrich D., Xoplaki E., Grosjean M., Wanner H. (2004) European seasonal
797 and annual temperature variability, trends, and extremes since 1500. Science, 303: 1499-
798 1503.
799 Millot R., Guerrot C., Vigier N. (2004a) Accurate and high precision measurement of lithium
800 isotopes in two reference materials by MC-ICP-MS. Geostandards and Geoanalytical
801 Research, 28: 53-159.
802 Millot R., C. Guerrot, T.D. Bullen (2004b) Precise measurement of Li isotopes by MC-ICP-
803 MS and comparison with TIMS analyses. Winter Conference on Plasma
804 Spectrochemistry, January 5-10, Fort Lauderdale, USA.
805 Millot R, Négrel Ph, Petelet-Giraud E (2007) Multi-isotopic (Li, B, Sr, Nd) approach for
806 geothermal reservoir characterization in the Limagne Basin (Massif Central, France)
807 Applied Geochemistry, 22: 2307-2325.
808 Miyata Y., Tokieda T., Amakawa H., Uematsu M., Nozaki, Y. (2000) Boron isotope variations
809 in the atmosphere. Tellus 52B, 1057-1065.
810 Négrel Ph., Lachassagne P., Laporte P. (1997) Caractérisation chimique et isotopique des
811 pluies de Cayenne (Guyane Francaise). C.R. Académie des Sciences 324, 379-386.
812 Négrel Ph., Roy, S. (1998) Chemistry of rainwater in the Massif Central (France) A Strontium
813 isotope and major element study, Applied Geochemistry 13: 941-952.

814 Négrel Ph., Guerrot C., Millot R. (2007) Chemical and strontium isotope characterization of
815 rainwater in France: influence of sources and hydrogeochemical implications. Isotopes in
816 Environmental and Health Studies, 43: 179-196.
817 Négrel Ph., Millot R., Brenot A. (2009) Lithium isotopes as a probe of groundwater circulation
818 in a peat land. 8th International Symposium on Applied Isotope Geochemistry, La Malbaie,
819 Canada.
820 Petelet-Giraud E., Casanova J., Chery L., Négrel Ph., Bushaert S. (2005) Attempt of isotopic
821 characterisation (delta O-18 and delta H-2) of present rainwater signature using lakes and
822 reservoirs: application to south-western France. Houille Blanche-Revue Internationale de
823 l'Eau, 2: 57-62.
824 Pistiner J.S., Henderson G.M. (2003) Lithium isotope fractionation during continental
825 weathering processes. Earth and Planetary Science Letters, 214: 327-339.
826 Plata-Bedmar A. (1994) Composicion isotopica de las precipitaciones y aguas subterraneas
827 de la Peninsula Iberica. Centro des Estudios de tecnicas Aplicadas, Madrid (Spain), 139p.
828 Pogge von Strandmann P.A.E., Burton K.W., James R.H., van Calsteren P., Gislason S.R.,
829 Mokadem F. (2006) Riverine behaviour of uranium and lithium isotopes in an actively
830 glaciated basaltic terrain. Earth and Planetary Science Letters, 251: 134-147.
831 Qi H.P., Coplen T.B., Wang Q.Z., Wang Y.H. (1997) Unnatural isotopic composition of lithium
832 reagents. Analytical Chemistry, 69: 4076-4078.
833 Rastogi N., Sarin M.M. (2005) Chemical characteristics of individual rain events from a semi-
834 arid region in India: Three-year study. Atmospheric Environment, 39: 3313-3323.
835 Razafindrakoto S. (1988) Teneurs en isotopes stables des précipitations et des eaux
836 souterraines et leurs variations en France. PhD Thesis, Université d'Avignon et des Pays
837 de Vaucluse, 341p.
838 Righi D., De Connick F. (1977) Mineralogic evolution in hydromorphic sandy soils and
839 podzols in "Landes du médoc", France. Geoderma, 19: 339-359.
840 Rozanski K., Araguas-Araguas L., Gonfiantini R. (1993) Isotopic patterns in modern global
841 precipitation. In Climate Change in Continental Isotopic Records. Geophysical Monograph
842 78, American Geophysical Union.
843 Rose-Koga E.F., Sheppard S.M.F., Chaussidon M., Carignan J. (2006) Boron isotopic
844 composition of atmospheric precipitations and liquid-vapor fractionations. Geochim.
845 Cosmochim. Acta, 70: 1603-1615.
846 Roy .S, Négrel Ph. (2001) A Pb isotope and trace element study of rainwater from the Massif
847 Central (France). Science of the Total Environment, 277, 225-239.
848 Schmitt A.D. Stille P. (2005) The source of calcium in wet anthropogenic deposit: Ca-Sr
849 isotope evidence, Geochimica et Cosmochimica Acta, 69: 3463-3468.

850 Schurch M., Kozel R., Schotterer U., Tripet J.P. (2003) Observation of isotopes in the water
851 cycle - the Swiss National Network (NISOT). Environmental Geology, 45: 1-11.
852 Teng F.Z., McDonough W.F., Rudnick R.L., Dalpé C., Tomascak P.B., Chappell B.W., Gao
853 S. (2004) Lithium isotopic composition and concentration of the upper continental crust.
854 Geochimica et Cosmochimica Acta, 68: 4167-4178.
855 Tomascak P.B. (2004) Developments in the Understanding and Application of Lithium
856 Isotopes in the Earth and Planetary Sciences. In Reviews in Mineralogy & Geochemistry,
857 55: 153-195.
858 Vigier N., Rollion-Bard C., Spezzaferri S., Brunet F. (2007) In-situ measurements of Li
859 isotopes in foraminifera. Geochemistry, Geophysics, Geosystems Q01003.
860 Widory D., Petelet-Giraud E., Négrel Ph., Ladouche B. (2005) Tracking the sources of nitrate
861 in groundwater using coupled nitrogen and boron isotopes: A synthesis. Environmental
862 Science & Technology, 39: 539-548.
863

Table caption

Table 1

Major cations and anions (Na, K, Mg, Ca, Cl, SO_4, NO_3, µmol/L), Li and B concentrations (µmol/L) and Li and B isotope compositions of rainwaters by location and sampling date. Rainfall amount (mm) and wind direction are also reported in this table. The prevailing wind direction data (in °) at each sample location were obtained from the Météo France database. Data reported for monthly average values in this table are weighted by the rainfall amount and only days with precipitation are considered.

Figure captions

Figure 1

Map of the rainwater sampling sites for lithium and boron isotopes (Brest, Dax, Orléans and Clermont-Ferrand). Graphs show the monthly mean rainfall amount (mm) at each site (modified from Négrel et al. 2007). Long-term monitoring stations for hydrogen and oxygen isotopes of the water molecule, at Thonon and Avignon, are also shown on this map.

Figure 2

2a: $\delta^{18}O$ vs. δD for all the monthly samples from the 5 long-term monitoring stations (Orléans, Brest, Dax, Thonon and Avignon. 2b: Annual weighted means of the same 5 stations. The Global Meteoric Water Line is also drawn (GMWL, $\delta D = 8 \times \delta^{18}O + 10$).

Figure 3

3a to 3e: $\delta^{18}O$ vs. δD for the monthly samples for each station. 3f: Mean weighted values for the period considered at each station. Blue diamonds correspond to individual data, red stars are the weight mean values and the grey dashed line is the Global Meteoric Water Line (GMWL) is $\delta D = 8 \times \delta^{18}O + 10$.

Figure 4

Cl concentrations in rainwaters (µmol/L) plotted as a function of the Na concentrations in rainwaters (µmol/L). The seawater dilution line and the linear relationship between Cl and Na are represented. A 95% confidence level is assigned to the data that falls between the two lines (modified from Négrel et al. 2007).

Figure 5

5a and 5b: Lithium and boron concentrations in rainwaters (µmol/L) vs. sodium concentrations in rainwaters (µmol/L). 5c: Lithium concentrations in rainwaters (µmol/L) plotted as a function of boron concentrations in rainwaters (µmol/L).

Figure 6

Histograms for $\delta^{7}Li$ and $\delta^{11}B$ (‰) values in rainwater samples.

Figure 7

7a and 7b: $\delta^{7}Li$ and $\delta^{11}B$ (‰) values plotted as a function of lithium and boron concentrations, respectively, in rainwaters (µmol/L).

Figure 8

Isovalue contour lines of the mean annual oxygen isotopic composition ($\delta^{18}O$) of rainwater in France. This map is based on rainwater, groundwater, lake (corrected for evaporation) and landsnail shell data. Contour lines from Spain (Plata-Bedmar 1994), Italy (Longinelli and Selmo 2003, Longinelli et al. 2006) and United Kingdom (Darling and Talbot 2003, Darling et al. 2003), together with Swiss data (Schurch et al. 2003) where also used to constrain lines at the French borders. The location of rainwater sampling stations for $\delta^{18}O$ vs. δD is also shown on this map (blue: short-term monitoring; red: long-term monitoring).

Figure 9

9a and 9b: $\delta^{7}Li$ and $\delta^{11}B$ (‰) values plotted as a function of rainfall amount (mm); 9c and 9d: and sampling month.

Figure 10

$\delta^{7}Li$ (‰) values and Li concentrations (µmol/L) plotted as a function of wind direction for each sampling site. Bold lines represent parameter trends as a function of wind direction.

Figure 11

$\delta^{11}B$ (‰) values and B concentrations (µmol/L) plotted as a function of wind direction for each sampling site. Bold lines represent parameter trends as a function of wind direction.

Figure 12

$\delta^{7}Li$ (‰) plotted as a function of $\delta^{11}B$ (‰) in rainwater samples.

Figure 13

Histograms for Li and B contribution of marine sea salts (%) in rainwater samples.

Figure 14

14a and 14b: Li and B isotopic compositions plotted as a function of Li and B contribution of marine sea salts in rainwater samples, respectively.

Figure 15

$\delta^{7}Li$ (‰) plotted as a function of the Na/Li molar ratio.

Figure 16

947 $\delta^{11}B$ (‰) plotted as a function of NO_3/B molar ratios. The anthropogenic end-member (urban
948 aerosols) is from Chetelat et al. (2009), the biomass-derived end-member is from Chetelat et
949 al. (2005) and the fertilizer end-member is from Widory (pers. comm.).
950

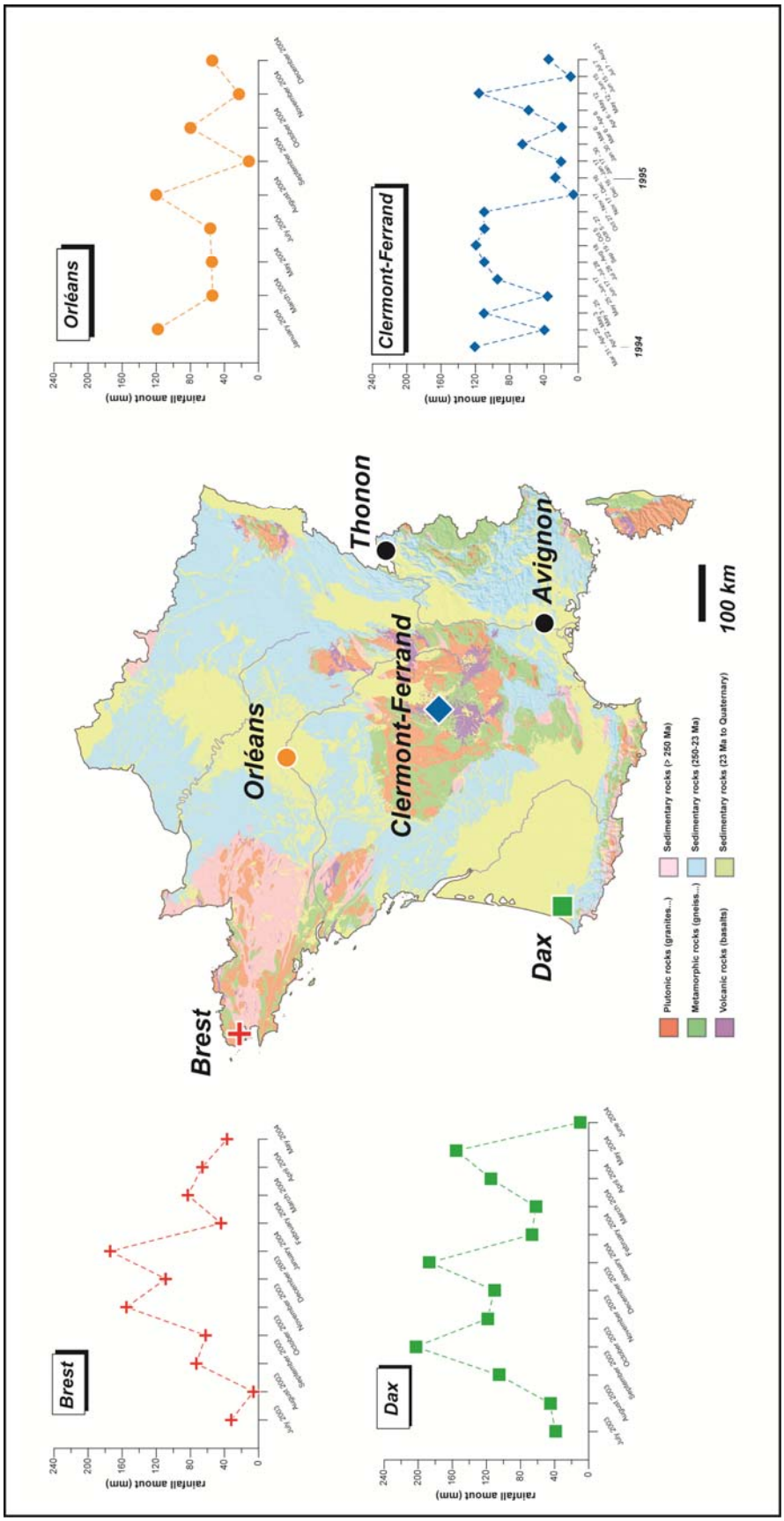
951
952
953
954

Table 1

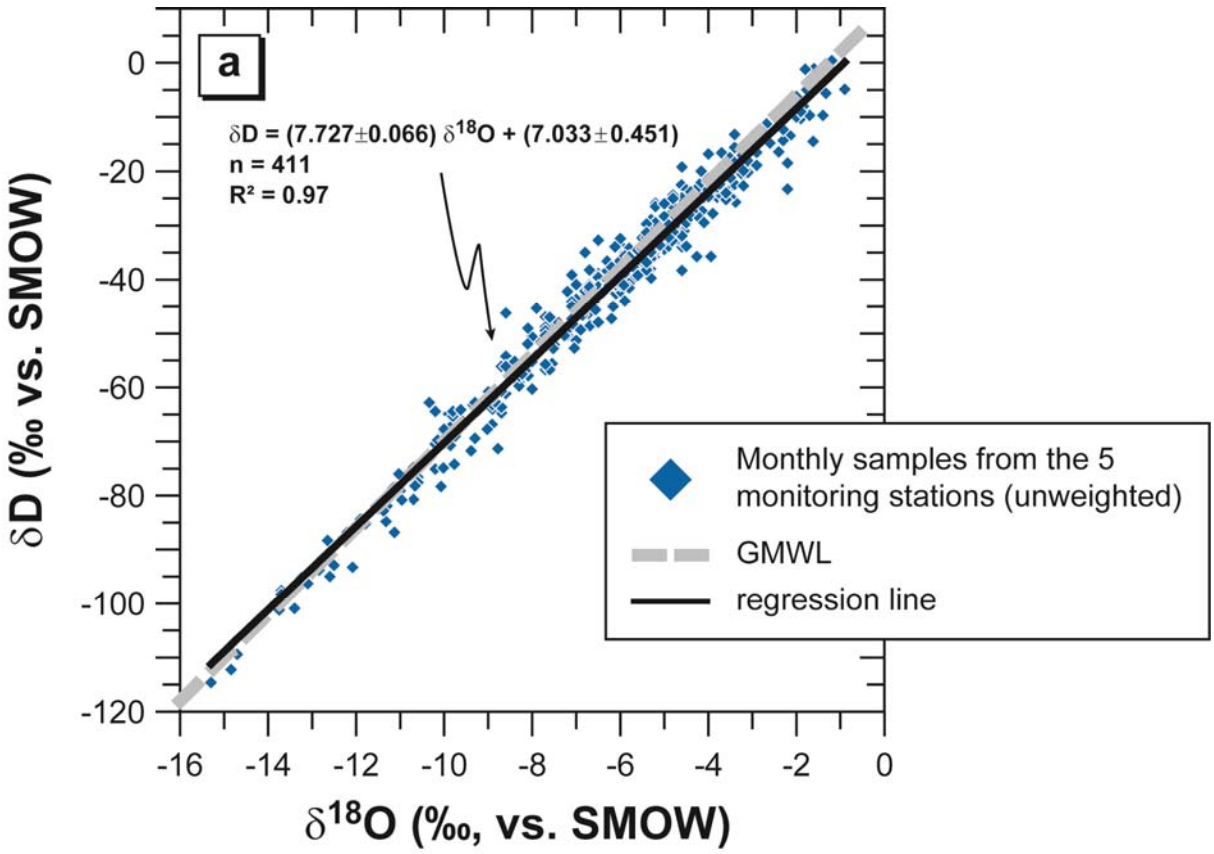
Location / Sampling date	Reference	Rainfall amount mm	Main Wind direction °	Na µmol/L	K µmol/L	Mg µmol/L	Ca µmol/L	Cl µmol/L	SO_4 µmol/L	NO_3 µmol/L	Li µmol/L	B µmol/L	δ^7Li ‰	$\delta^{11}B$ ‰
BREST														
July 2003	03-E-524	32	223	117.5	5.8	16.1	8.5	117.7	21.3	36.7	0.051	0.398	23.4	35.1
August 2003	03-E-525	6	105	235.0	31.9	62.8	65.8	228.6	113.9	172.0	0.142	3.793	19.3	27.5
September 2003	03-E-526	73	176	74.3	2.8	10.9	7.9	75.2	22.3	68.9	0.051	0.262	15.1	38.1
October 2003	03-E-527	62	193	208.3	5.6	23.8	11.4	218.9	32.2	58.9	0.052	0.329	22.2	39.6
November 2003	03-E-528	155	129	142.6	4.0	17.2	6.0	150.1	23.2	16.7	0.053	0.207	17.7	40.3
December 2003	03-E-529	109	174	292.7	7.6	33.1	6.2	322.3	31.3	32.1	0.060	0.298	27.2	40.6
January 2004	04-E-52	174	232	231.7	5.1	25.7	7.0	243.1	25.5	6.8	0.050	0.214	28.6	40.1
February 2004	04-E-53	44	57	393.8	10.3	47.8	15.9	450.1	46.0	36.0	0.059	0.355	26.3	37.8
March 2004	04-E-54	83	209	346.2	11.0	40.6	12.6	390.4	42.3	47.0	0.042	0.449	25.8	39.5
April 2004	04-E-55	66	150	227.7	4.8	27.6	10.2	236.3	39.3	57.8	0.033	0.357	22.7	37.5
May 2004	04-E-56	37	234	323.9	10.7	39.5	12.6	366.2	42.1	80.3	0.045	0.599	19.4	35.2
DAX														
July 2003	03-E-164	39	256	204.3	63.6	24.4	55.2	156.6	43.9		0.069	1.013	34.1	15.9
August 2003	03-E-165	45.4	248	89.5	9.2	14.9	33.8	50.7	40.8	49.7	0.078	1.167	21.5	7.9
September 2003	03-E-166	105.4	225	196.1	14.3	18.0	23.2	176.3	32.5	2.6	0.087	0.717	21.1	12.9
October 2003	03-E-147	203.1	207	273.6	50.2	26.9	57.8	272.3	33.8	110.6	0.077	1.174	25.2	8.3
November 2003	03-E-148	118.7	238	155.7	15.9	15.2	25.7	136.6	24.8	-	0.062	0.830	19.8	2.0
December 2003	03-E-149	110.7	230	194.2	11.5	16.9	44.6	167.0	30.6	2.9	0.058	0.595	21.0	11.8
January 2004	03-E-150	187.3	242	176.4	9.3	16.9	20.8	164.8	25.9	-	0.047	0.997	23.0	7.1
February 2004	03-E-151	66.8	212	203.9	51.0	29.6	49.2	198.3	44.9	28.7	0.058	0.369	23.5	19.8
March 2004	03-E-152	62.1	210	137.4	41.9	27.1	64.5	135.5	36.9	3.5	0.055	0.662	17.2	9.4
April 2004	03-E-153	115.1	255	255.2	53.8	33.7	65.0	247.3	18.3	3.0	0.068	1.099	18.9	7.9
May 2004	03-E-154	155.1	243	160.1	10.9	19.8	31.4	163.7	23.5	-	0.050	0.898	22.8	7.8
June 2004	03-E-155	10.2	268	108.3	26.8	22.8	114.4	113.5	42.0	-	0.079	1.340	25.3	26.5
ORLEANS														
January 2004	04-E-46	118	221	38.7	6.9	5.8	8.9	32.7	8.4	-	0.041	0.029	13.0	29.8
March 2004	04-E-48	54	231	61.4	11.3	10.8	21.4	49.6	22.6	39.4	0.055	0.408	14.2	13.1
May 2004	04-E-50	55	243	52.4	17.0	8.2	12.7	39.4	14.1	9.5	0.046	0.818	19.2	6.0
July 2004	04-E-295	57	220	53.4	13.5	12.0	23.3	30.4	21.0	-	0.068	1.987	11.2	-0.3
August 2004	04-E-296	120	267	34.5	6.6	11.6	21.0	16.6	14.0	-	0.057	2.430	9.2	-2.4
September 2004	04-E-297	11.5	234	96.9	19.4	22.8	39.4	98.3	27.9	-	0.081	6.184	19.4	-3.3
October 2004	04-E-298	80	175	59.0	14.4	8.9	12.9	41.7	16.5	12.9	0.038	1.246	14.3	0.0
November 2004	04-E-299	23	219	92.3	60.5	13.3	17.8	66.8	39.5	59.0	0.052	0.281	22.9	22.7
December 2004	04-E-300	54	201	51.0	17.8	6.3	9.4	50.1	13.0	19.8	0.036	0.217	21.9	9.8
CLERMONT-FERRAND														
March 31 - April 22 1994	PSM1	120	288	39.1	4.1	4.4	12.3	39.4	51.0	74.6	0.049	0.312	77.6	11.9
April 22 - May 3 1994	PSM2	40	173	6.1	4.1	2.1	10.5	7.0	23.4	16.7	0.041	0.156	6.7	22.9
May 3 - 25 1994	PSM3	110	239	3.9	2.6	1.7	8.0	7.0	16.1	34.1	0.004	0.116	8.7	28.7
May 25 - June 17 1994	PSM4	37	256	9.1	7.2	0.2	14.8	16.9	19.8	-	0.075	0.191	4.9	25.0
June 17 - July 28 1994	PSM5	95	256	20.0	23.8	4.3	79.0	31.0	47.9	42.9	-	-	-	-
July 28 - August 18 1994	PSM6	110	243	4.8	3.3	0.9	16.0	16.9	33.3	30.2	0.033	0.248	6.7	32.8
September 19 - October 5 1994	PSM7	120	294	4.3	2.3	1.9	16.8	7.9	7.1	12.7	0.027	0.106	9.0	32.0
October 5 - 27 1994	PSM8	110	152	8.7	2.6	0.8	15.0	10.1	7.3	-	0.027	0.050	14.7	19.5
October 27 - November 17 1994	PSM9	110	172	0.4	13.6	6.3	1.0	13.5	4.2	-	-	-	-	-
November 17 - December 16 1994	PSM10	5	246	6.5	3.8	6.3	9.5	13.0	36.6	53.8	-	-	-	-
December 16 1994- January 17 1995	PSM11	28	197	32.2	1.8	8.3	12.0	44.2	21.6	38.7	0.044	0.172	63.8	27.2
January 17 - 30 1995	PSM12	20	195	8.7	3.1	5.8	3.3	14.1	6.1	-	0.041	0.104	33.2	25.4
January 30 - March 6 1995	PSM13	65	214	43.0	2.3	4.0	5.8	21.7	13.2	19.0	0.292	0.520	95.6	4.8
March 6 - April 6 1995	PSM14	20	258	23.0	5.1	3.2	12.3	25.4	14.2	17.5	-	-	-	-
April 6 - May 12 1995	PSM15	58	302	8.3	4.1	2.3	11.0	11.8	39.4	47.0	0.022	0.160	3.2	19.8
May 12 - June 15 1995	PSM16	115	229	8.7	4.9	2.6	18.0	-	-	-	0.044	0.226	7.8	25.2
June 15 - July 7 1995	PSM17	10	124	4.8	9.0	-	12.0	37.5	13.9	69.2	0.037	0.239	8.3	26.8

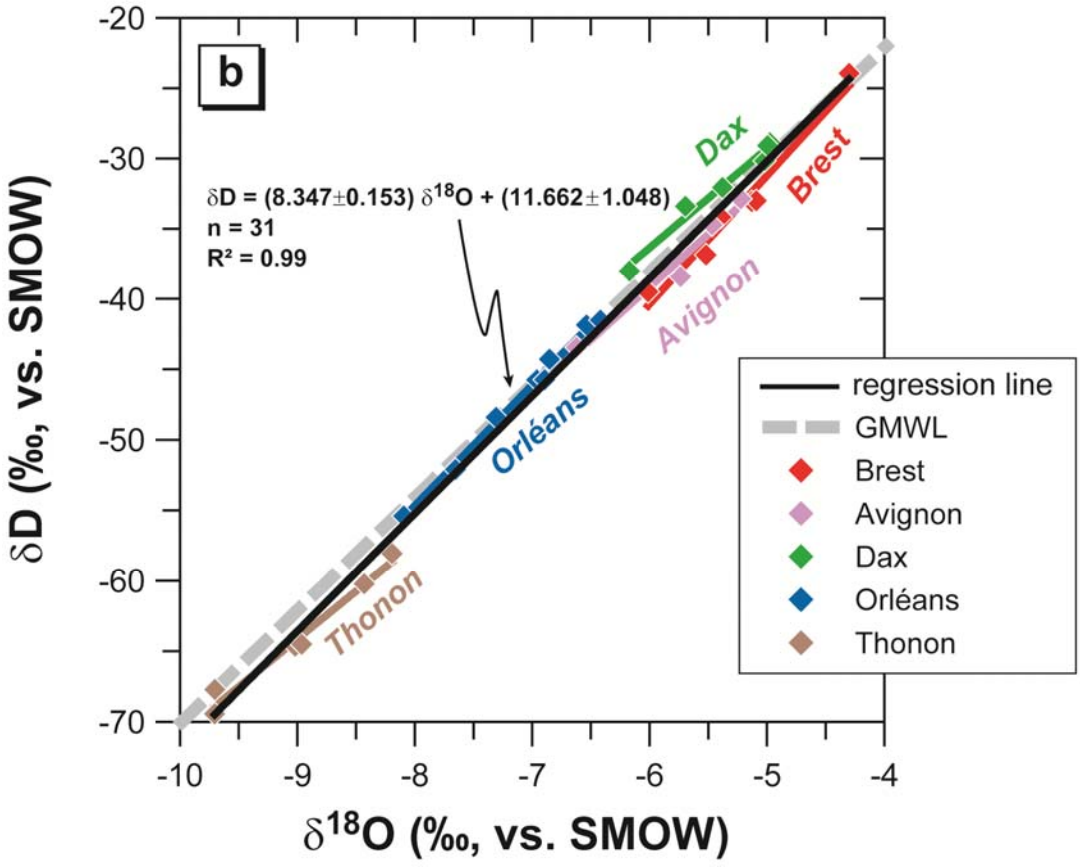
955
956

Figure 1


Orléans
Clermont-Ferrand
1994
1995
rainfall amout (mm)
Thonon
Avignon
Orléans
Clermont-Ferrand
Brest
Dax
100 km
Plutonic rocks (granites...)
Metamorphic rocks (gneiss...)
Volcanic rocks (basalts)
Sedimentary rocks (> 250 Ma)
Sedimentary rocks (250-23 Ma)
Sedimentary rocks (23 Ma to Quaternary)
Brest
Dax

960 **Figure 2**
961





962

Figure 3

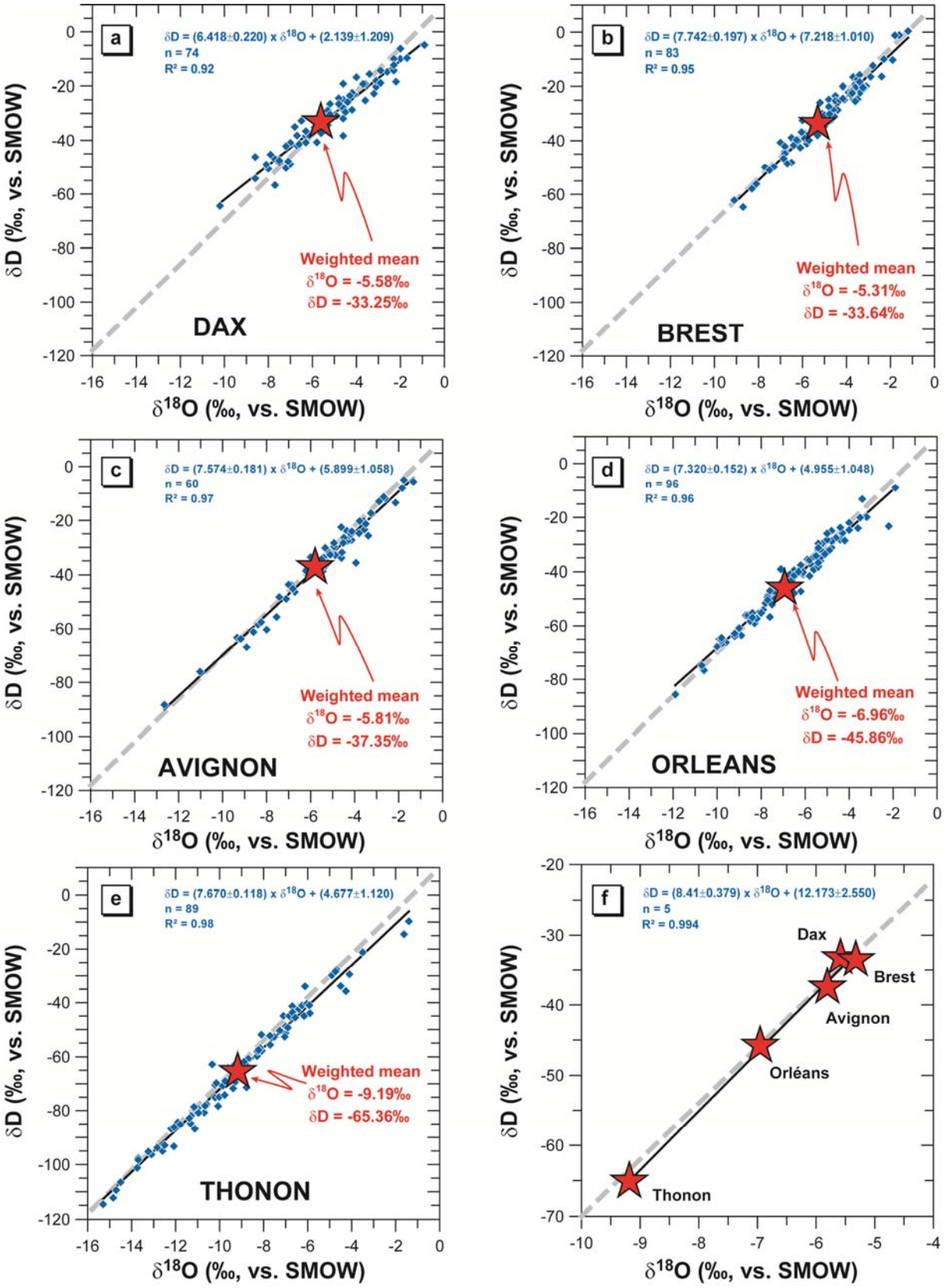

a
δD = (6.418±0.220) x δ18O + (2.139±1.209)
n = 74
R² = 0.92
Weighted mean
δ18O = -5.58‰
δD = -33.25‰
DAX
b
δD = (7.742±0.197) x δ18O + (7.218±1.010)
n = 83
R² = 0.95
Weighted mean
δ18O = -5.31‰
δD = -33.64‰
BREST
c
δD = (7.574±0.181) x δ18O + (5.899±1.058)
n = 60
R² = 0.97
Weighted mean
δ18O = -5.81‰
δD = -37.35‰
AVIGNON
d
δD = (7.320±0.152) x δ18O + (4.955±1.048)
n = 96
R² = 0.96
Weighted mean
δ18O = -6.96‰
δD = -45.86‰
ORLEANS
e
δD = (7.670±0.118) x δ18O + (4.677±1.120)
n = 89
R² = 0.98
Weighted mean
δ18O = -9.19‰
δD = -65.36‰
THONON
f
δD = (8.41±0.379) x δ18O + (12.173±2.550)
n = 5
R² = 0.994
Dax
Brest
Avignon
Orléans
Thonon
δD (‰, vs. SMOW)
δ18O (‰, vs. SMOW)

Figure 4

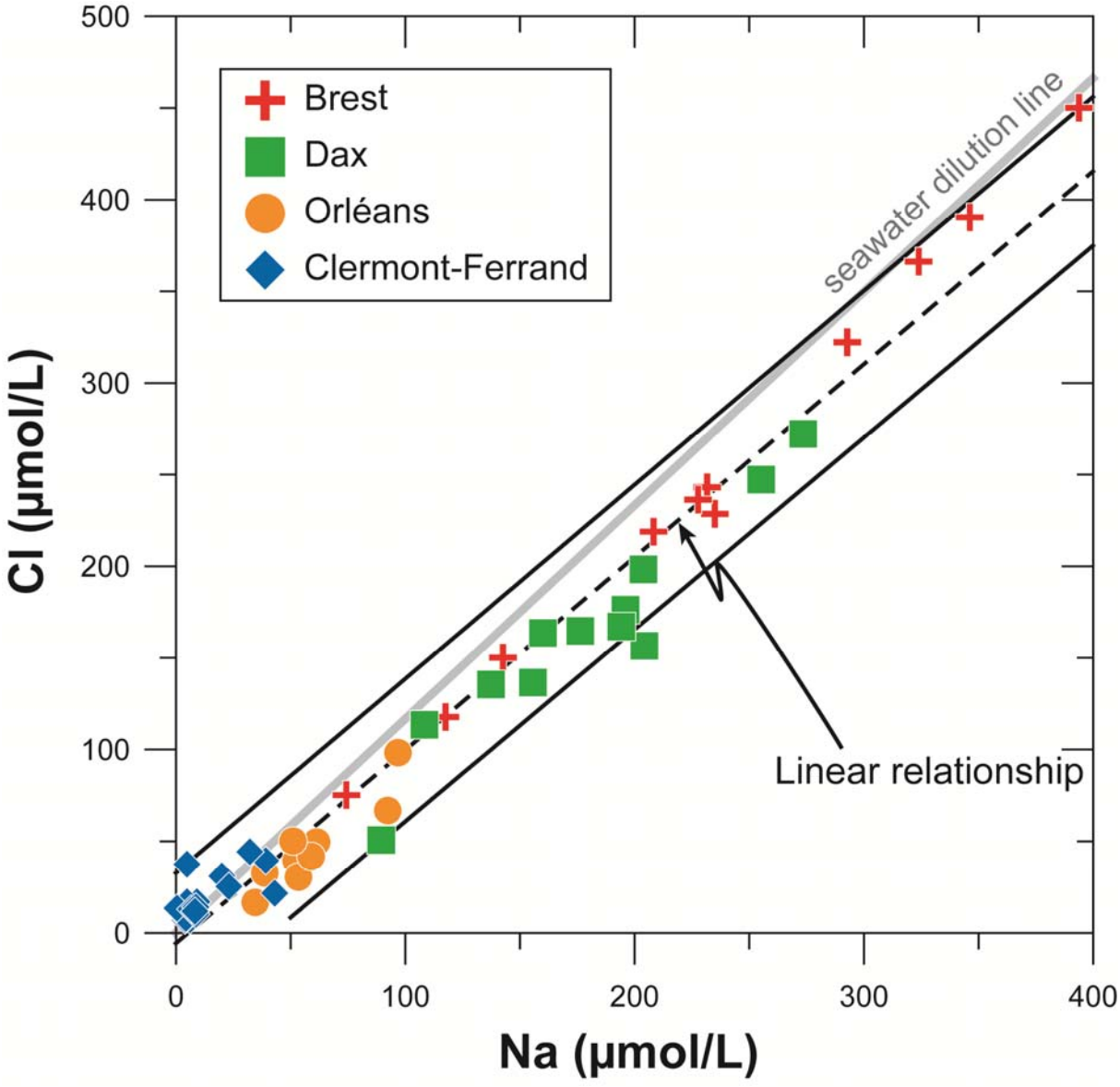
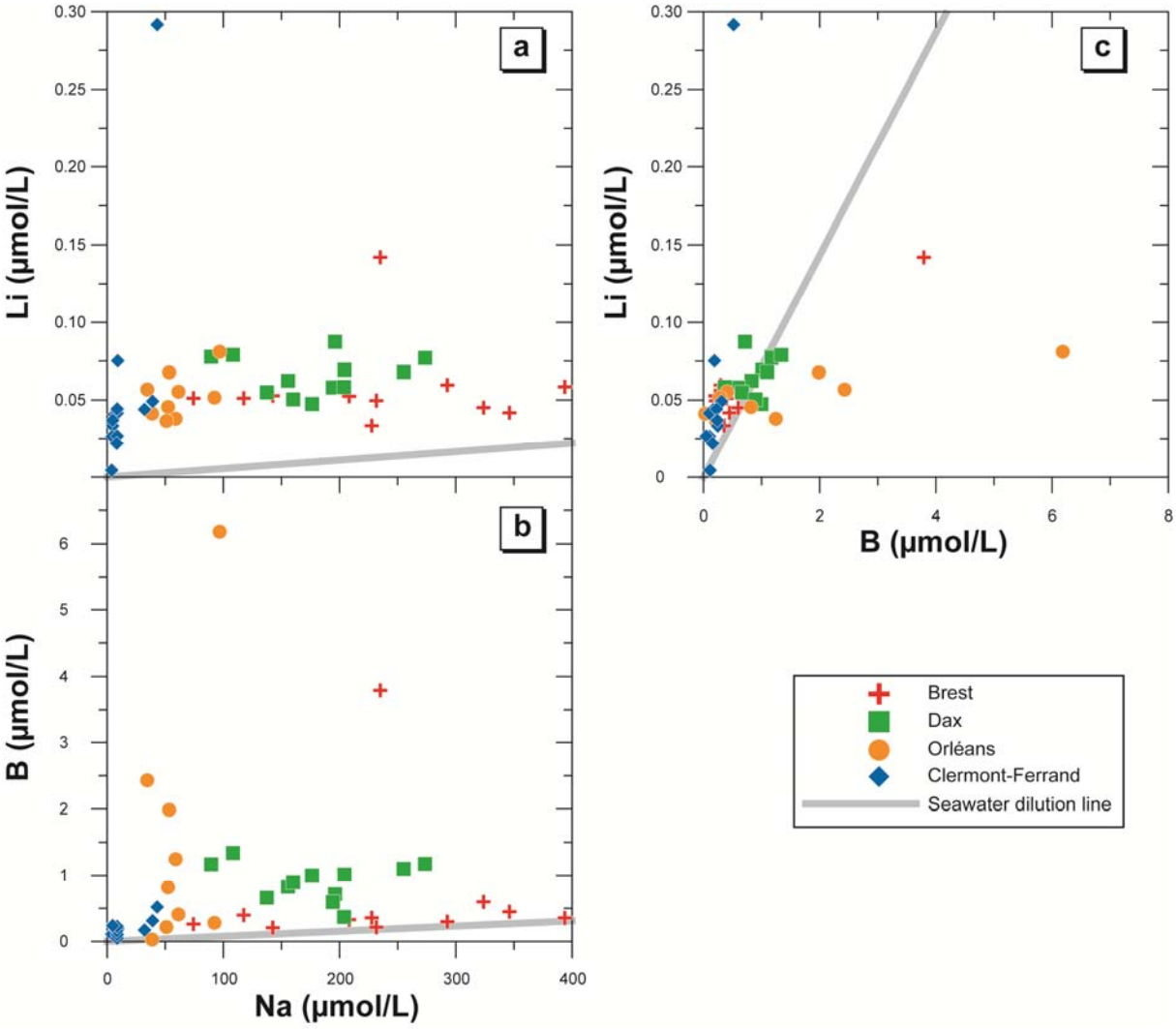
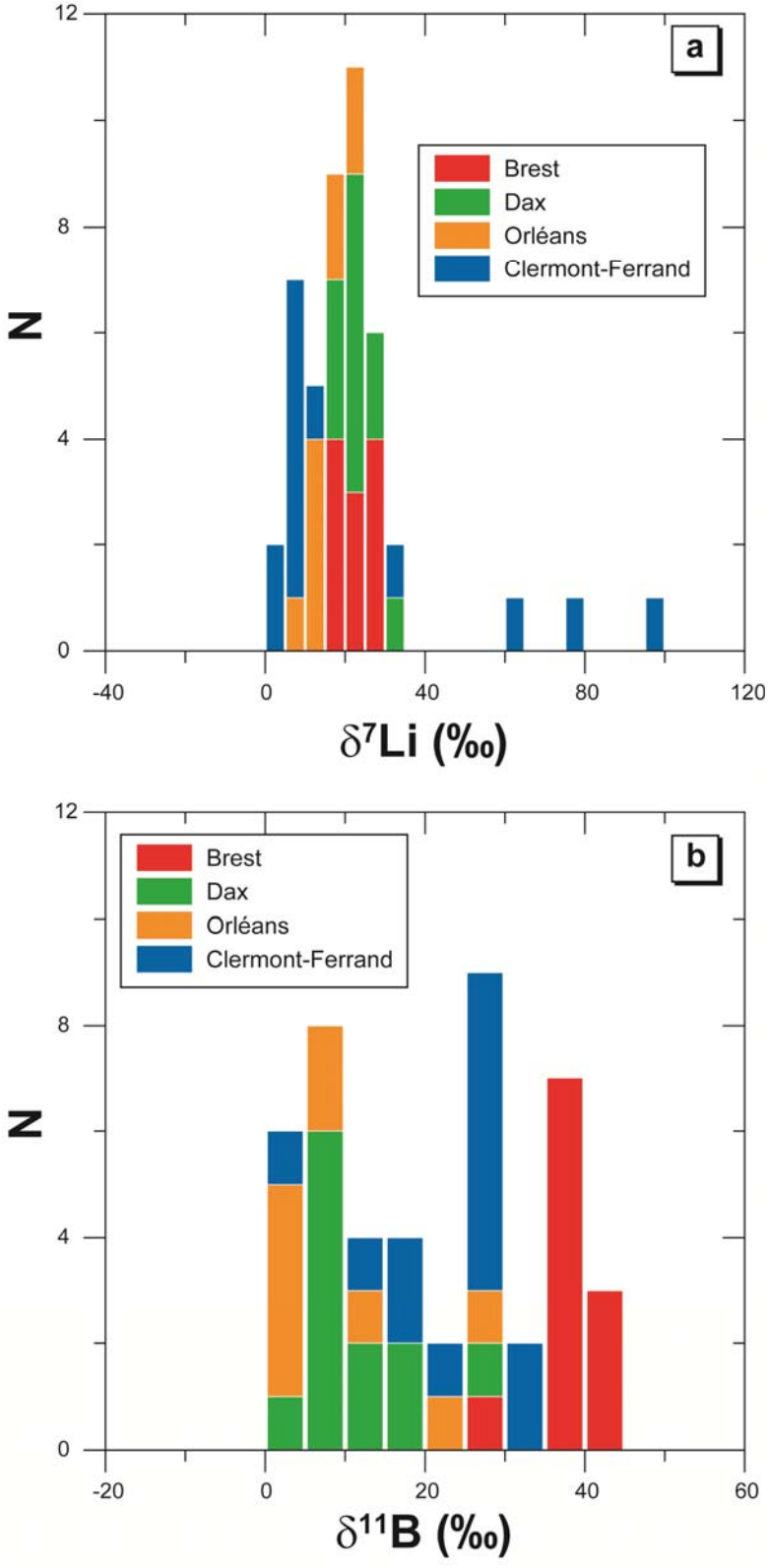

Brest
Dax
Orléans
Clermont-Ferrand
seawater dilution line
Linear relationship
Cl (µmol/L)
Na (µmol/L)
0
100
200
300
400
500

Figure 5

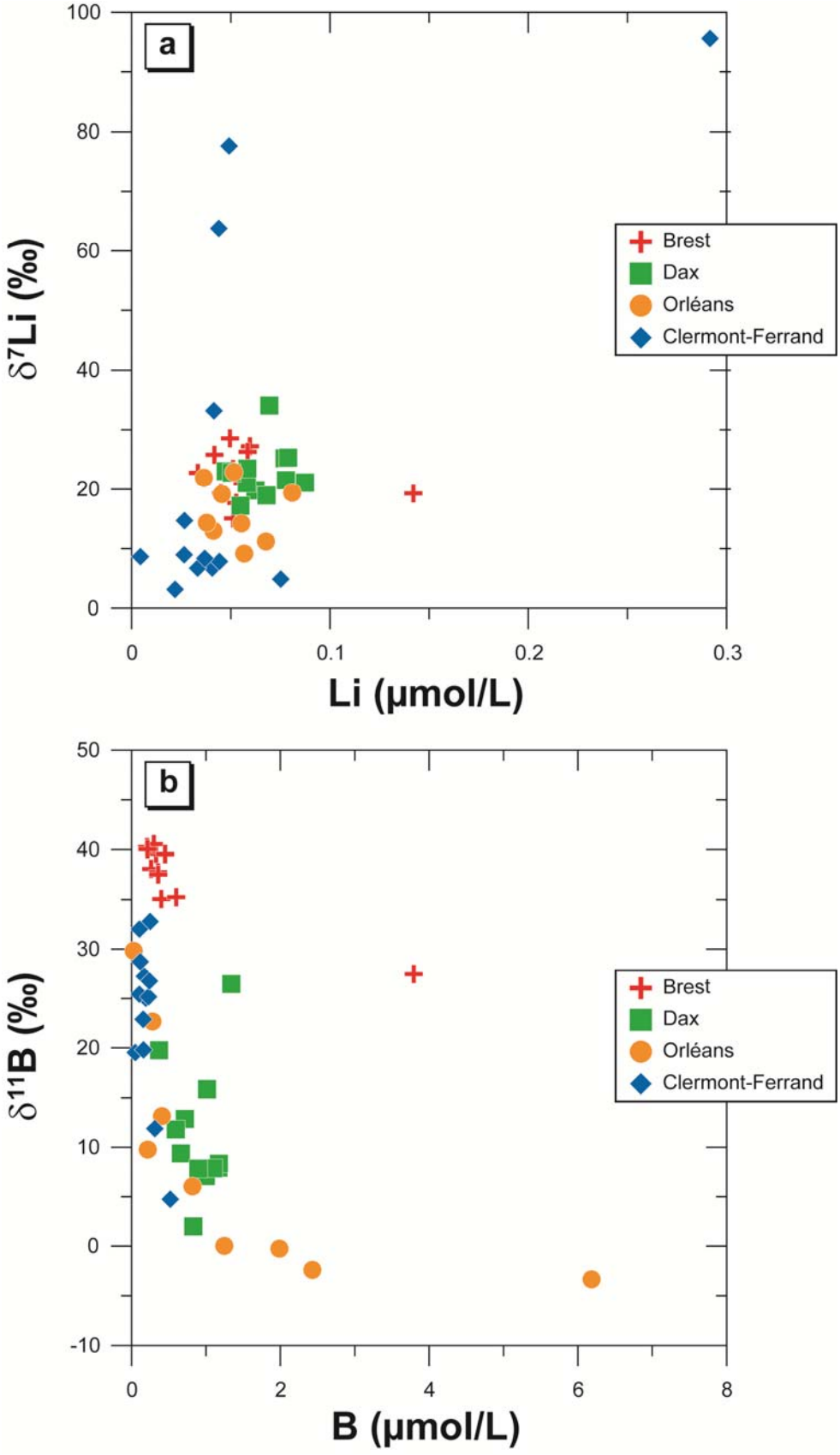

a
b
c
Li (µmol/L)
B (µmol/L)
Na (µmol/L)
Li (µmol/L)
B (µmol/L)
Brest
Dax
Orléans
Clermont-Ferrand
Seawater dilution line

988 **Figure 6**



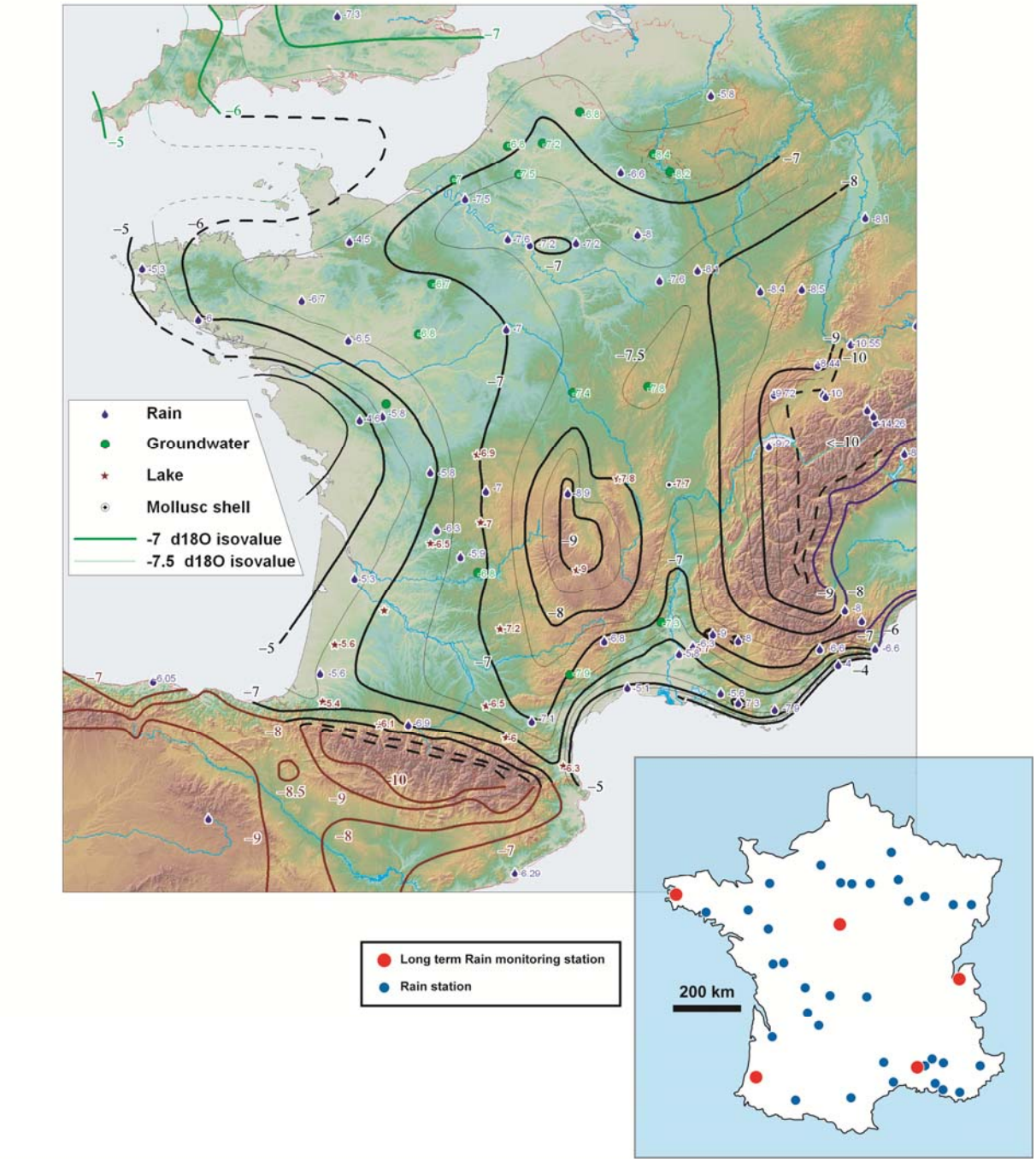
989

990 **Figure 7**



991

992 **Figure 8**
993



994

Figure 9

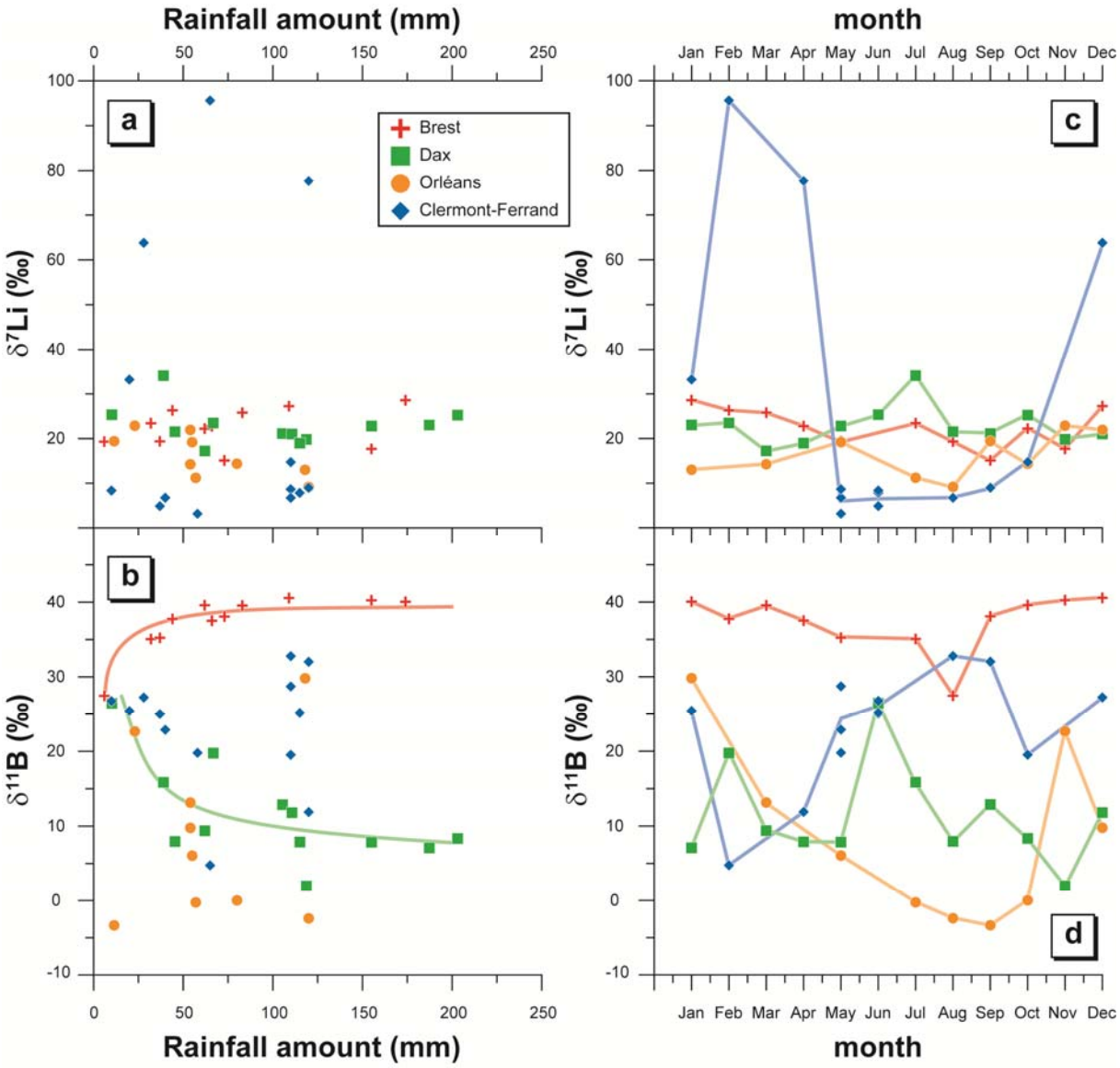
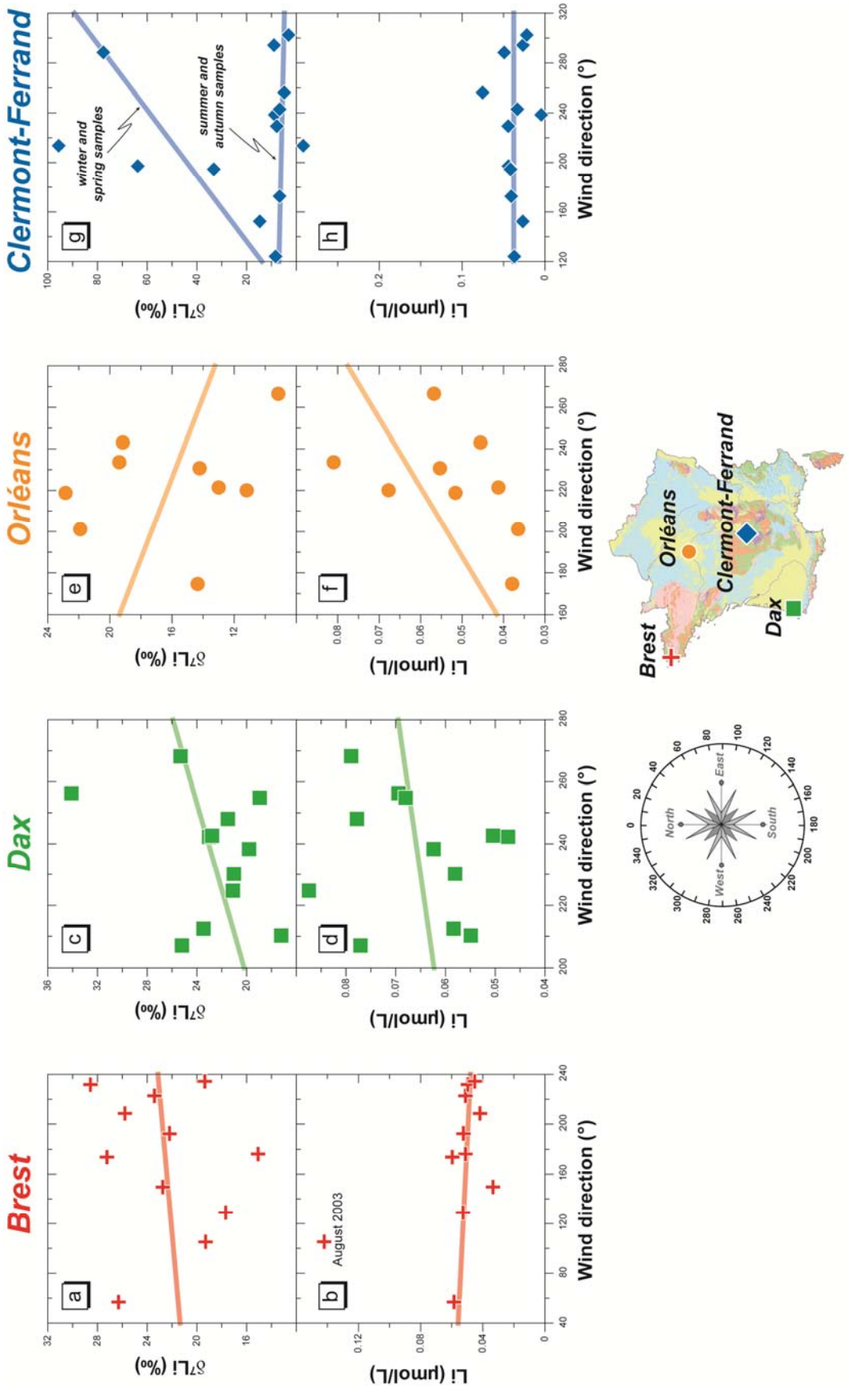
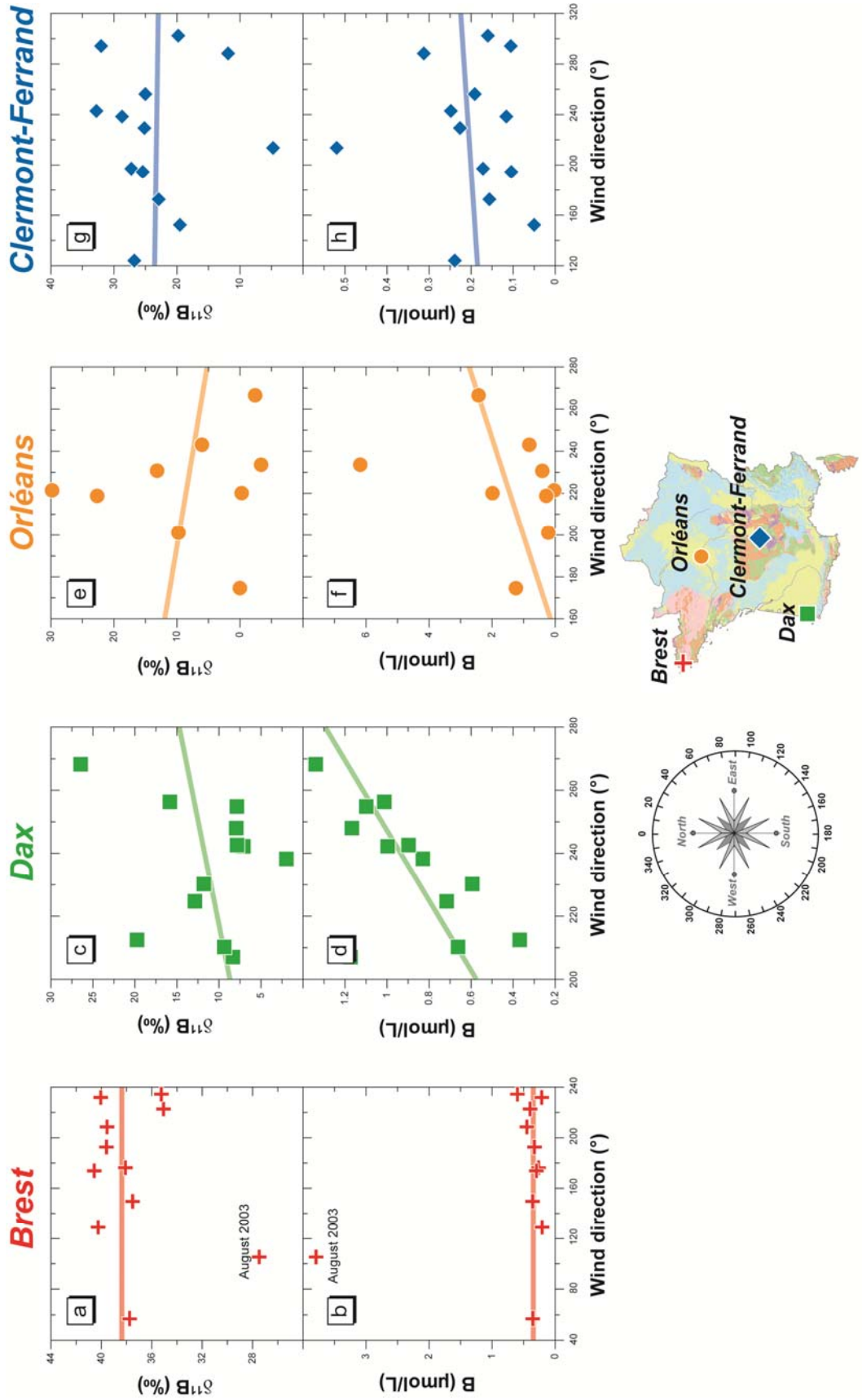

Rainfall amount (mm)
month
a
b
c
d
Brest
Dax
Orléans
Clermont-Ferrand
δ7Li (‰)
δ11B (‰)
Jan Feb Mar Apr May Jun Jul Aug Sep Oct Nov Dec

Figure 10

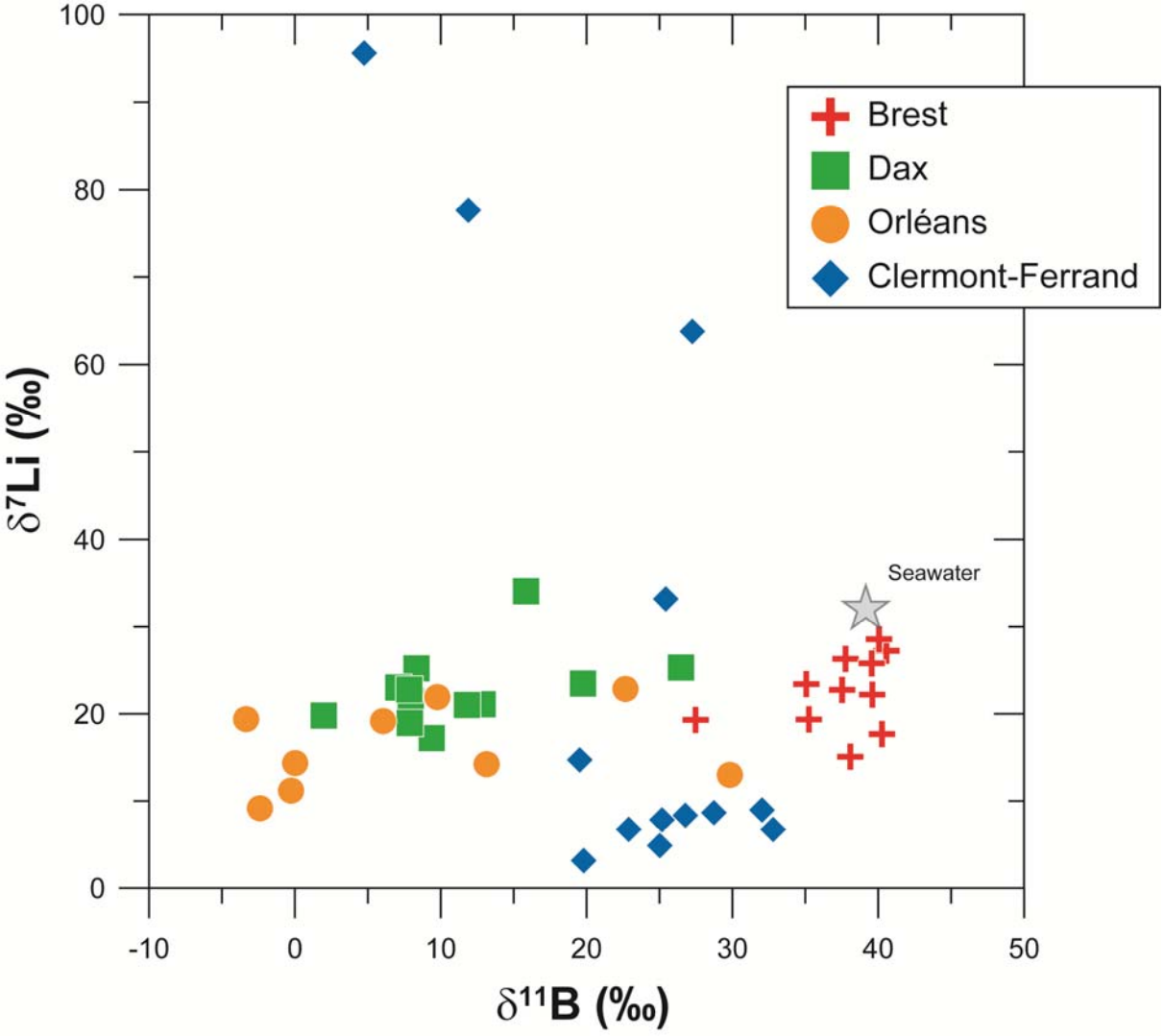

Brest
Orléans
Clermont-Ferrand
Dax
a
b
c
d
e
f
g
h
August 2003
winter and spring samples
summer and autumn samples
Wind direction (°)
Li (µmol/L)
North
East
South
West

1010 **Figure 11**
1011

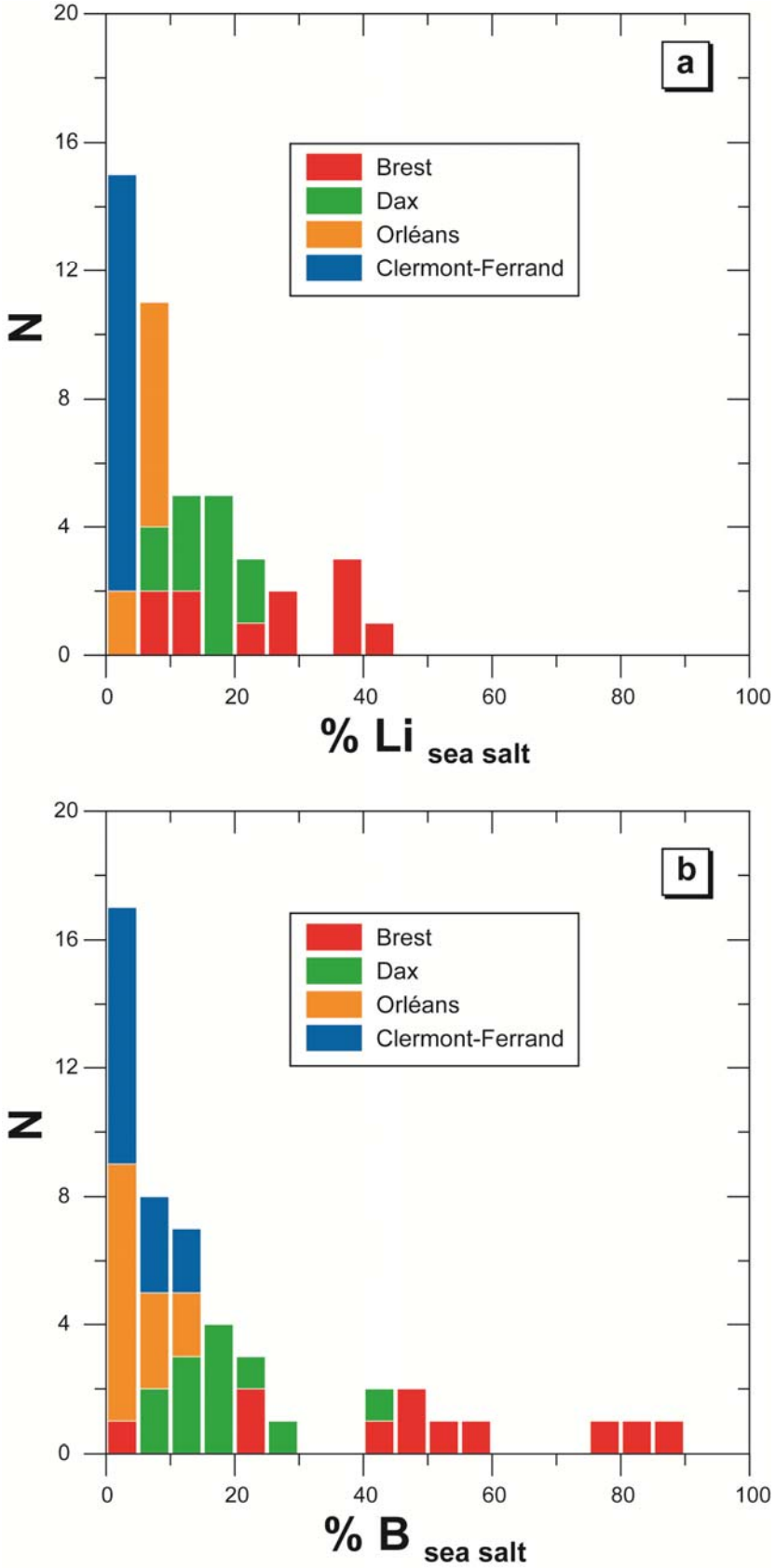


1012

Figure 12


Brest
Dax
Orléans
Clermont-Ferrand
Seawater
δ7Li (‰)
δ11B (‰)
100
80
60
40
20
0
-10
0
10
20
30
40
50

1023 **Figure 13**



1024
1025

Figure 14

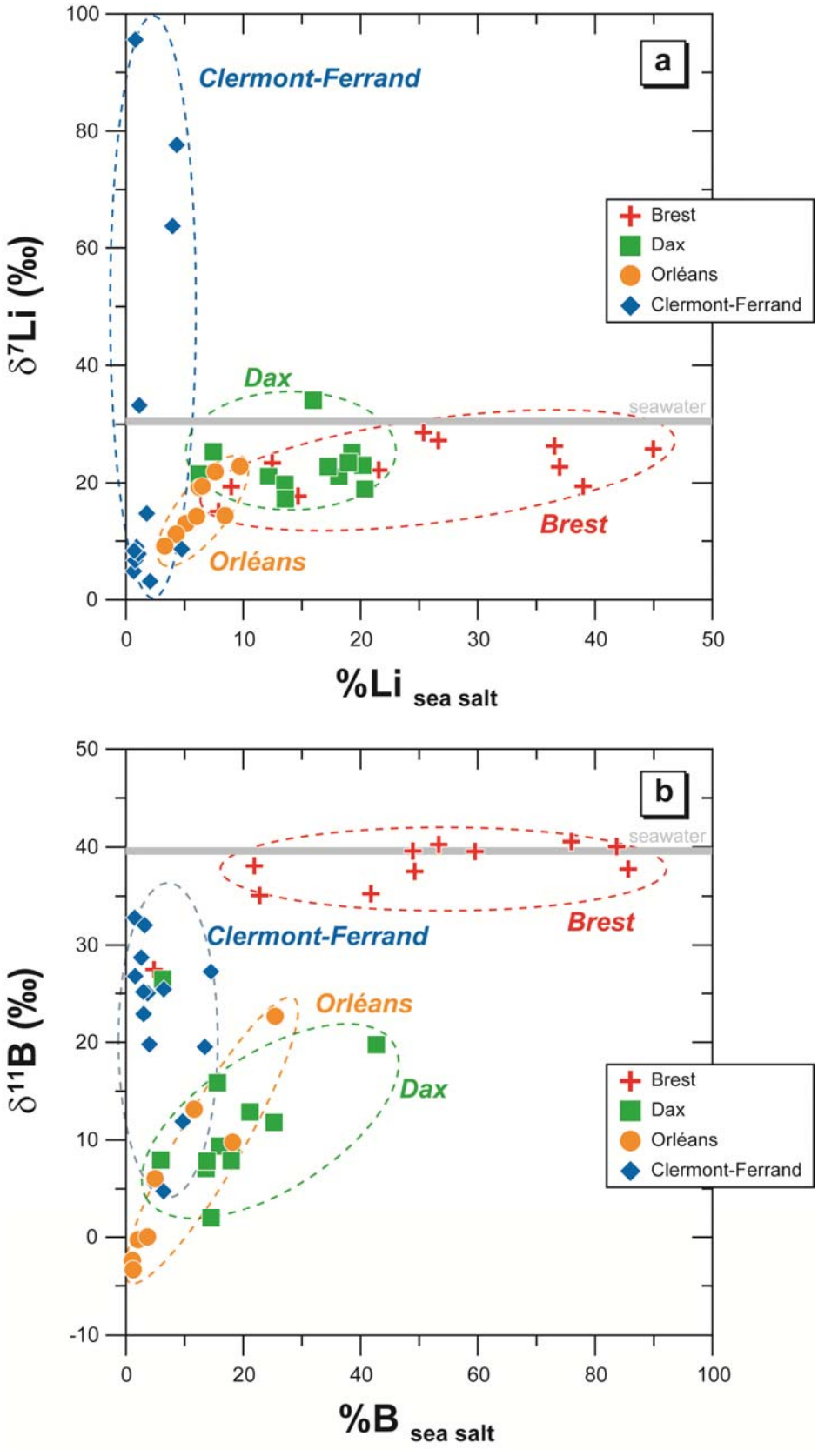

a
Clermont-Ferrand
Dax
Orléans
Brest
seawater
Brest
Dax
Orléans
Clermont-Ferrand
δ7Li (‰)
%Li sea salt
b
seawater
Brest
Clermont-Ferrand
Orléans
Dax
Brest
Dax
Orléans
Clermont-Ferrand
δ11B (‰)
%B sea salt

Figure 15

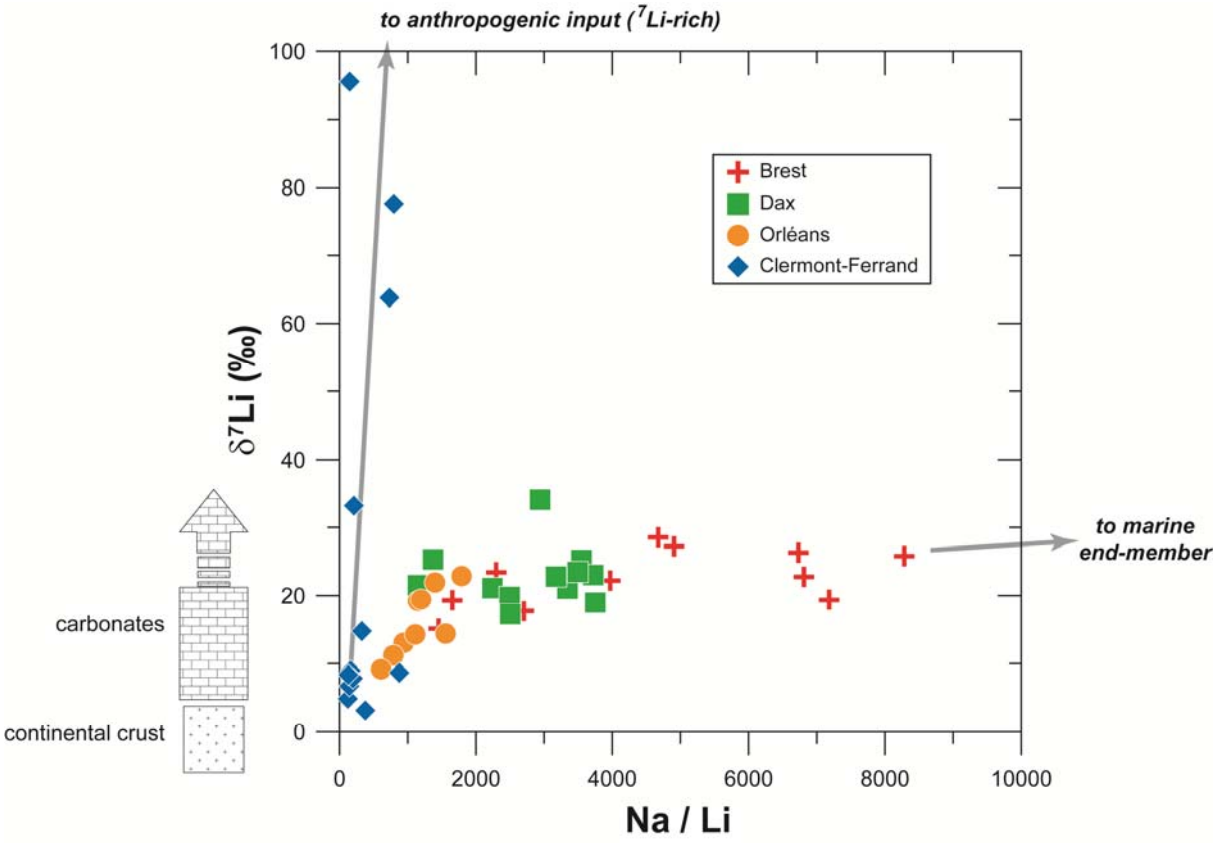
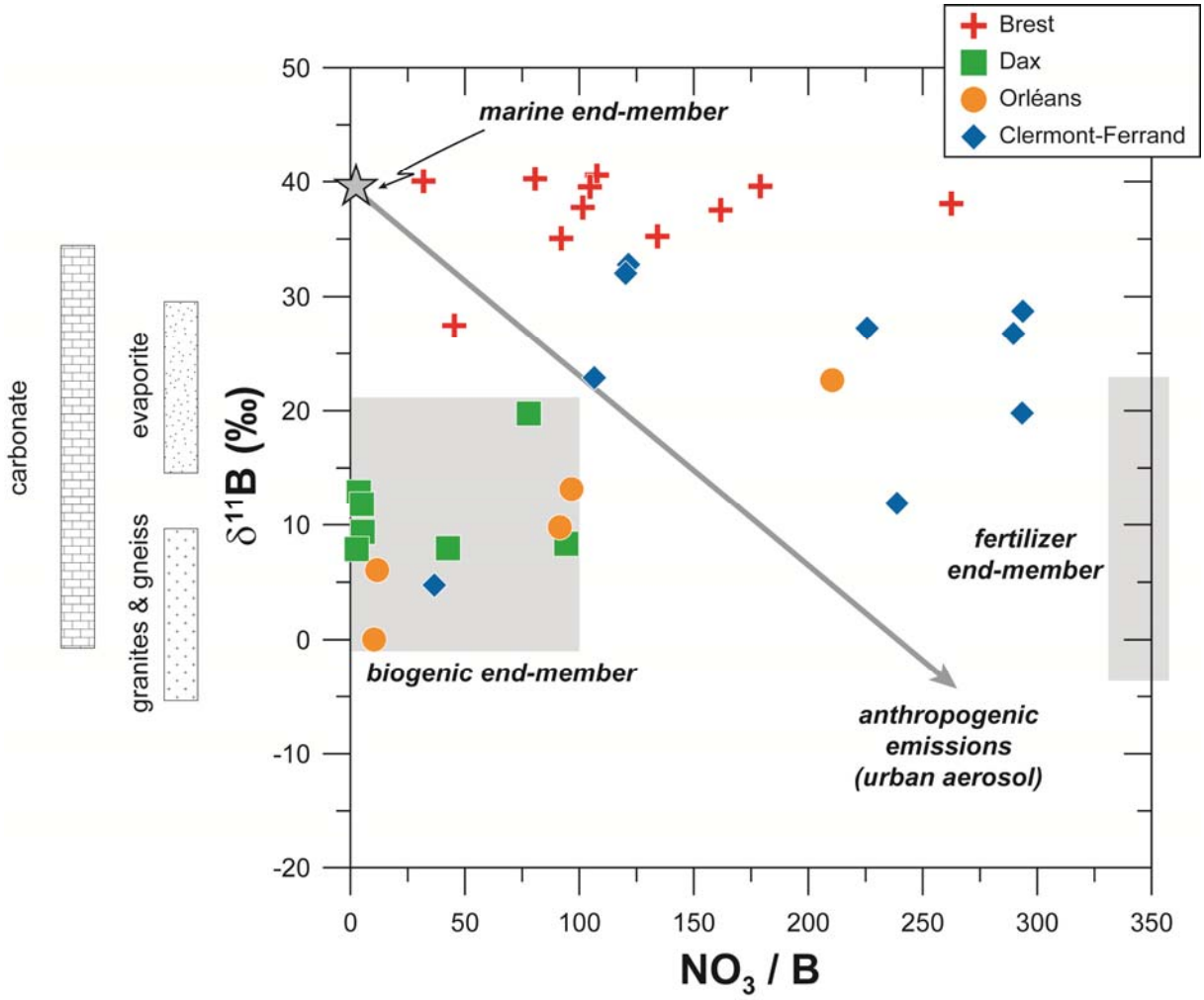

to anthropogenic input (^{7}Li-rich)
100
80
60
40
20
0
δ^7Li (‰)
Brest
Dax
Orléans
Clermont-Ferrand
to marine
end-member
carbonates
continental crust
0
2000
4000
6000
8000
10000
Na / Li

Figure 16


Brest
Dax
Orléans
Clermont-Ferrand
marine end-member
fertilizer
end-member
biogenic end-member
anthropogenic
emissions
(urban aerosol)
carbonate
evaporite
granites & gneiss
δ11B (‰)
NO3 / B
50
40
30
20
10
0
-10
-20
0
50
100
150
200
250
300
350